PERFORMANCE IMPROVEMENT IN A CIRCUIT BREAKER MECHANISM

`

DISSERTATION

submitted in partial fulfillment of the requirements
for the degree of

MASTER OF ENGINEERING

IN

CAD/CAM ENGINEERING

by

Manuj Arora

Roll No: 801281012

Under the guidance of

Mr. Deosharan Roy
Sr. Manager – Technology
Global R & D Centre
Crompton Greaves Limited
Mumbai – 400042

Dr. S.P. Nigam
Visiting Professor, MED
Thapar University, Patiala
Punjab – 147004

MECHANICAL ENGINEERING DEPARTMENT
THAPAR UNIVERSITY
PATIALA – 147004, INDIA

JULY - 2014

CERTIFICATE

This is to certify that the thesis entitled **"PERFORMANCE IMPROVEMENT IN A CIRCUIT BREAKER MECHANISM"** submitted by **Mr. Manuj Arora** to the **Thapar University, Patiala** towards partial fulfillment of the requirements for the award of the Degree of Master of Engineering in **CAD/CAM Engineering** is a bona fide record of the work carried out by him under our supervision and guidance. The contents of this thesis, in full or in parts, have not been submitted to any other Institute or University for the award of any degree or diploma.

11/7/2014

Mr. Deosharan Roy
Sr. Manager – Technology
CG Global R & D Center
Crompton Greaves Ltd.
Mumbai – 400042

Dr. S.P. Nigam
Visiting Professor
Mech. Engg. Department
Thapar University
Patiala – 147004

Countersigned By:

Dr. Ajay Batish
Professor and Head
Mech. Engg. Department
Thapar University
Patiala – 147004

Dr. S.K. Mohapatra
Senior Professor and DOAA
Mech. Engg. Department
Thapar University
Patiala – 147004

i

DECLARATION

"I hereby declare that this submission is my own work and that, to the best of my knowledge and belief, it contains no material previously published or written by another person nor material which has been accepted for the award of any other degree or diploma of the university or other institute of higher learning, except where due acknowledgment has been made in the text.

Place : PATIALA

Date : 18/07/2014

MANUJ ARORA

801281012

ABSTRACT

Main design criterion for a circuit breaker is quick and timely disconnection and reconnection of different parts for protection and control. A sluggish response can stress the network thus causing damage to the equipments in a substation. In this study, performance of gas insulated circuit breaker has been improved by minimizing the wipe time of operation. A rigid multi body dynamic simulation model was created in SOLID WORK. All the possible parameters that could influence the wipe time were identified and their effects on the same were further studied. A reduction of 15.8 % in the wipe time and an equivalent reduction of 22.9% in the opening time were reported from the simulated results.

Further effect of flexibility of insulating pull rod (made of FRP tube) on travel curve of the contacts was also studied and it was found that flexibility in the pull rod has to be considered for correct prediction of travel characteristics of the circuit breaker contacts. An effort was made to measure the elastic constant of the insulating pull rod and study the effect of improved stiffness on the opening time.

ACKNOWLEDGEMENT

The research work related to this thesis has been carried out at **Crompton Greaves, Global R&D Centre, Kanjurmarg, Mumbai**. My experience with Crompton Greaves has been incredible where I have been given unique opportunities.

Firstly, I would like to thank **Dr. S.P.Nigam,** visiting professor, Department of Mechanical Engineering, for recommending me to Crompton Greaves. It has been a great pleasure for me to work under his guidance.

I am deeply grateful to my research advisor, **Mr. Deorsharan Roy,** Technology Manager, Crompton Greaves for providing excellent guidance, encouragement and inspiration throughout the project work. Without his invaluable teaching, this work would never have been a successful one.

Special thank to **Mr. Srinivas D** and **Mr. Suresh Rajan,** from CG management team for offering me to work on this project at Crompton Greaves.

Dozens of people have helped and taught me immensely at Crompton Greaves. I am extremely thankful to each one of them. Special thanks to my team member Kunal, Dharamraj, Vijendra, Santosh, Ketan and Sangram.

Sincere thanks to **Dr. S.K. Mohapatra**, Senior Professor and DOAA.

I express my gratitude to **Dr. Ajay Batish**, Professor and Head, Department of Mechanical Engineering, **Dr. R.S. Kaler**, Dean Resource Planning and Generation, faculty member and staff of Department of Mechanical Engineering for extending all possible help in carrying out the dissertation work directly or indirectly. I praise the help provided by all my friends.

Last but not least, I acknowledge my sincere gratitude to my parents for their constant encouragement and support.

TABLE OF CONTENTS

CHAPTER 3 PROBLEM DEFINATION

CHAPTER 4 DYNAMICS OF CIRCUIT BREAKER

CHAPTER 5 PARAMETRIC MODELLING AND ANALYSIS FOR WIPE TIME

LIST OF TABLES

LIST OF FIGURES

ABBREVIATIONS

SF6	:	Sulfur hexafluoride
EHV	:	Extra high voltage
O	:	Opening
C	:	Closing
kV	:	kilovolt
PE	:	Power Electronic
DC	:	Direct current
GCB	:	Gas circuit breaker
AC	:	Alternating current
CIGRE	:	International Council on Large Electric Systems
MATLAB	:	Matrix laboratory
MBD	:	Multi body dynamics
MSL	:	Main shaft lever
BCL	:	Bell Crank Lever
FEA	:	Finite element analysis
FRP	:	Fiber reinforced plastics
UTM	:	Universal testing machine
IEC	:	International Electrotechnical Commission

ABAQUS

SOLID WORKS PREMIUM

CHAPTER 1

INTRODUCTION TO CIRCUIT BREAKER

1.1. OVERVIEW

With the expansion of civilization, consumption for electric power is steadily increasing and will continue to grow in the coming decades. Newer concepts of power generations have been developed which deals with very high level of voltages. Hence there is a need for a reliable transmission and distribution system. The circuit breakers which forms the part of transmission and distribution system are the ultimate safety devices and play a vital role in the protection and control in an electric power system. Demand for the performance of these high voltage circuit breakers has increased and there is further scope of development in the circuit breaker technology.

1.2. CIRCUIT BREAKER

A circuit breaker is a device which is used to protect an electrical circuit from damage caused by overload or short circuit. Its basic function is to detect a fault condition and interrupt current flow. Unlike a fuse, which operates once and then must be replaced, a circuit breaker can be reset (either manually or automatically) to resume normal operation

Circuit breakers can be made in varying sizes, from small devices that protect an individual household appliance up to large switchgear designed to protect high voltage circuits feeding an entire city. Figure 1 and 2 below shows some images of circuit breaker.

Figure 1: A two-pole miniature circuit breaker

Figure 2: Circuit breaker for 145kV (L) and 420 kV (R)

For maintenance or repair of electrical equipment and transmission lines, the circuit breakers will disconnect the electrical equipment and transmission lines from voltage source and hence will ensure personnel safety. Figure 3 shows an arrangement of circuit breaker in a transmission lines.

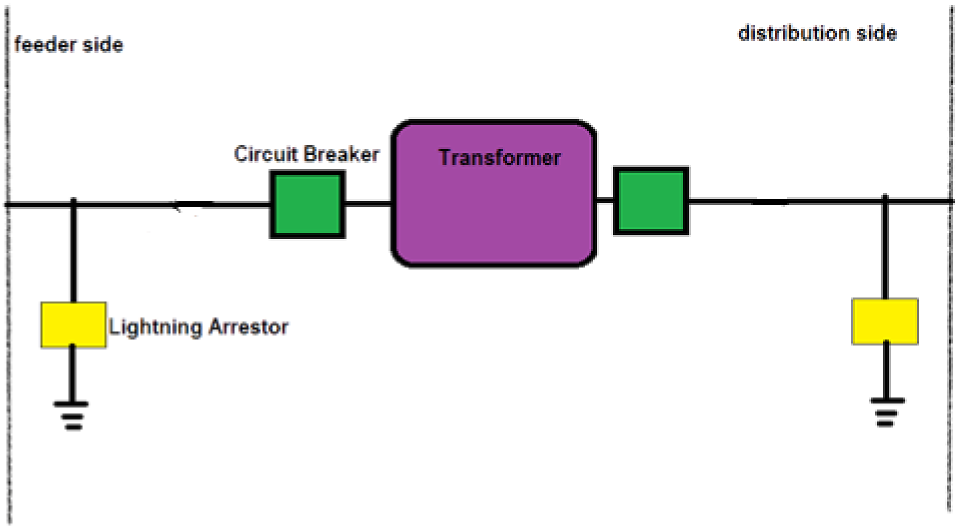

Figure 3: General Layout of Circuit breaker in a transmission line

1.3. COMPONENTS OF CIRCUIT BREAKER

Major components of Circuit breaker are

1. Interrupter or breaking unit
2. Support insulator
3. Support Structure
4. Operating mechanism
5. Primary terminals

Figure 4 shows all these components.

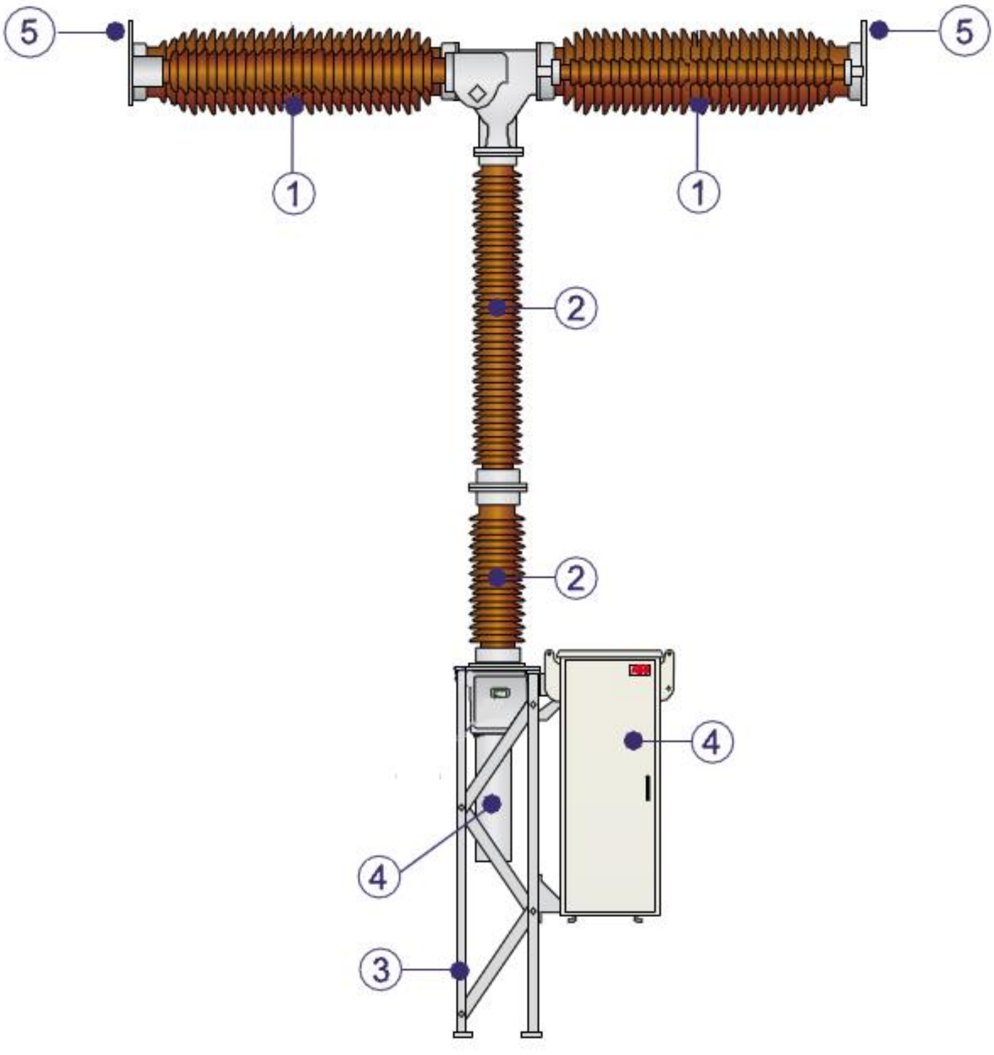

Figure 4: Components of high voltage circuit breaker

1.3.1. INTERRUPTER

It is a portion in a circuit breaker where current conduction and interruption in the power circuit occurs. It is closed volume where opening and closing of contacts takes place.

Under normal operation, circuit breaker is in closed position as shown in figure 5a. However when the opening command is actuated, moving contact starts moving with respect to fixed contact. During separation of contacts, the medium between the contacts gets highly ionized and it glows in the form of arc. Current continues to flow through this path even though the contacts are physically separated.

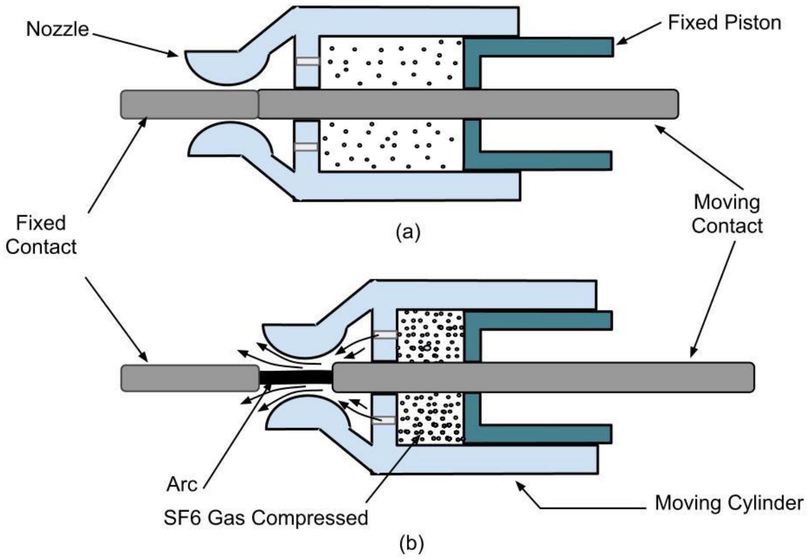

Figure 5: Puffer type SF6 Circuit Breaker

As long as this arc is sustained in between the contacts, the current continues to flow through the circuit breaker and does not get interrupted because arc is nothing but ionization of a gas and hence conductive path of electricity. For total interruption of current in the circuit breaker, it is essential to quench/cool and extinguish the arc as quick as possible. The main designing criteria of a interrupter is to provide appropriate technology of arc quenching in circuit breaker to fulfill quick and safe current interruption. Generally SF6 gas in enclosed in a chamber which provides the following function

a. It provides sufficient insulation between the contacts when circuit breaker opens.
b. It extinguishes the arc occurring between the contacts when circuit breaker opens.

Some of the properties of SF6 gas that make its use in power applications desirable are high dielectric strength, unique arc quenching ability, excellent thermal stability, and good thermal conductivity. Opening of contacts in an interrupter is executed in the following steps stationary

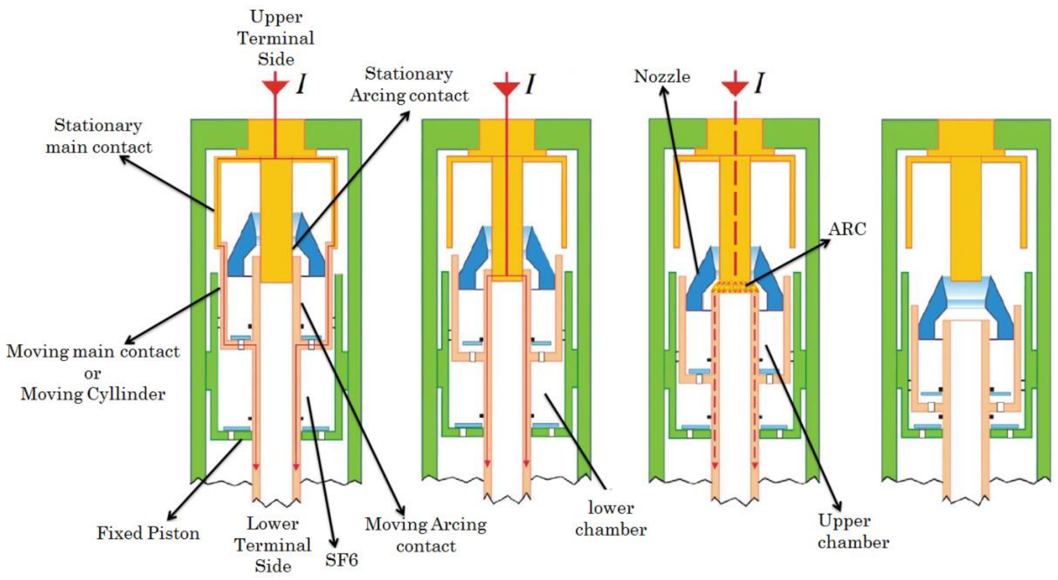

Figure 6: Steps for opening operation

Step1: Under Normal operating condition, Circuit breaker is in closed position and current always flow through the main contact systems as shown in the first picture of figure 6.

Step2: Opening command is actuated; moving cylinder moves downwards thus separating the main contacts. However arcing contacts does not get separated and current keeps flowing from the upper terminal to lower terminal through the arcing contacts as shown in the second picture of figure 6. During the down stroke, moving cylinder exerts a pressure on the SF6 gas housed in the lower chamber; the pressure increase generated in the lower chamber opens the connection valve of the upper chamber. The compressed gas flows from the lower to the upper chamber thus equalizing the pressures. Refer second picture of figure 6.

Step3: Arcing contacts gets separated and arc is generated between the fixed and moving arcing contact. Current keeps flowing due to the asrc generated between the fixed and moving arcing contacts. The gas cannot leak from the nozzle as the hole is blocked by the fixed contact or from the inside of the moving contact because of the arc clogging effect. Refer third picture of figure 6.

Step4: The arc is quenched; the lower chamber reaches its minimum volume and its maximum pressure level. As the self-generated pressure of the dead volume decreases, due to the outflow of the gas through the moving contacts, the valve re-opens. From now on, a new jet of fresh gas flows in and makes the temperature of the contacts fall. At the same time, the gas flows through the nozzle, free from the fixed arcing contact. The "cleaning" of the arcing chamber by means of fresh gas makes the device suitable for another reclosing and the interruption up to the maximum breaking capacity. Refer fourth picture of figure 6.

Therefore in any SF6 high voltage circuit breaker, Interrupter has 2 contacts system

a. Main contact systems
b. Arcing contact system

The main contact conducts the normal operating currents and the arcing contacts are used to take the load off the main contacts when the circuit breaker opens and closes. This will protect the main contacts from getting burned. The arc created when the arcing contact gets separated is extinguished at one of the next zero crossings of current. The heat from the arc causes a sudden rise in pressure between the arcing contact system and the piston. It is from here that hot SF6 gas is blasted to extinguish the arc at the zero crossing.

1.3.2. OPERATING MECHANISMS

Energy is required for the motion of the moving contacts with respect to fixed contact. This energy needs to be provided by some mechanism that can drive the moving contact so as to close and open the circuit breaker. The mechanism required for driving the moving contact is of great importance as long as closing and opening of connection is achieved through mechanical motion.

Any EHV circuit breaker has 2 Operating mechanisms, one mechanism for closing the contacts (current conduction) and another mechanism for opening the contacts (current interruption).The requirements of operating mechanisms are as follows

a. Close the circuit breaker and keep it in closed position.
b. Open the circuit breaker and keep it in open position.

As per requirement, opening and closing commands are given spontaneously to the circuit breaker without any warning which poses a serious requirement for the operating mechanism.

1.3.2.1. OPPOSING FORCES

List of opposing forces that act during operating mechanism are given as

a. Electromagnetic Forces between contacts

Electromagnetic forces exist only during closing operation. During closing operation when contact touches, electromagnetic forces appear. Magnitude of these forces is proportional to square of the current where as direction is opposite to the direction of motion of moving contact during closing operation. These forces are large during short circuit conditions. Operating mechanism should overcome these forces and close the circuit breaker.

b. Inertia of the moving subassembly

Inertia forces occur because of masses of the component.

c. SF6 gas pressure

Compressed SF6 gas, used for quenching the arc exerts pressure on the face of moving cylinder and needs to be taken into account.

d. Static and Dynamic Friction

Mechanism consists of series of linkages connected by revolute and sliding joints. Friction exists between pair of linkages connected by revolute and sliding joints and needs to be taken into consideration

e. Damping force

It provides opposing force to stop the linkage after completion of close / open operation.

1.3.2.2. PARAMETERS FOR MECHANISM DESIGN

Parameters that need to be considered for mechanism design are listed as

a. Voltage rating:

This decides the minimum distance between contacts in open condition. From this consideration stroke of mechanism can be finalized. Higher the voltage rating for breaker; higher will be stroke of the mechanism & higher the mechanism energy requirement. For e.g. In a 400 kV, GCB, mechanism stroke is 1.5 times the stroke for 145 kV GCB.

b. Current rating

This settles the size / cross section of contacts, which in term determines the mass of contact. The temperature rise limits have direct influence on the contact size.

c. Short-circuit rating

During short circuit conditions, electromagnetic forces are generated at contacts. When, breaker is required to close and latch against these forces, the mechanism has to provide sufficient energy to close against the opposing forces independent of closing speed or momentum of moving parts achieved by a high speed during closing stroke. Higher the short circuit making current, higher will be opposing electromagnetic force.

d. Mechanical Duty

Circuit Breaker should perform Open-Close-Open sequence (O - 0.3 s - CO) without external supply to mechanism. After close operation, Circuit Breaker should be able to perform open operation without any internal delay. According to IEC 62271-100, for rapid auto-reclosing operating duty cycle is O - 0.3 s - CO - 3 min - CO. The time of 3 min is the time needed for the operating mechanism to restore its power after O - 0.3 s - CO.

e. Rated Break time

Break time refers to the time when there is complete opening of contacts. For lesser the break time requirement, contact system has to be accelerated faster which requires higher mechanism energy. Hence for 2 cycle breaker, higher energy mechanism is needed. This also calls for faster trip coil operations & lesser de-latching time in the mechanism.

1.3.2.3. TYPES OF MECHANISM

Different possible operating mechanisms for EHV circuit breakers are

a. Pneumatic
b. Hydraulic
c. spring according to its power source
d. Power electronics
e. Combination of above

Heinemann [ ] presented a comprehensive comparison of different operating mechanisms technologies linked to high voltage interrupters. Table 1 presents some of the features of different types operating mechanism

	Pneumatic	Hydraulic	Spring	Power Electronics	Hydro-mechanical
Energy Storage	Gas pressurized		Springs	DC capacitor	Springs
Release of Energy	Valve		Mechanical latch	PE switch	Valve
Transmission of Energy	Pneumatic Piston	Hydraulic piston	Linkage	Cables, copper plates	Hydraulic piston
Damping	Internal gas	Internal hydraulic	External hydraulic	PE switch	Internal hydraulic
Number of moving parts	Small		Medium	Minimum	Small
Maintenance requirements	Frequent		Some	Minimum	
Population	High, mainly high energy level		Very high, mainly low energy level	Low (new technology)	High, whole energy range
Technology trend	Phase out technology		Common technology	New Technology	Common Technology

Table 1: Types of Mechanism

The discussion is restricted to spring operated mechanisms.

Spring Mechanism:

A spring operated mechanism is one driven by mechanical energy stored in springs. The most common arrangement consists of two springs as shown in figure 7. Spring which is used for closing the connection is referred as closing spring while the spring which is used for opening the connection is referred as opening spring. The closing spring is mechanically charged by a motor and is held in the charged position (Completely compressed) by a Latch. When the closing signal releases this Latch, the spring drives the breaker to close, and in the same motion it charges the opening spring. Another Latch holds the breaker in the closed position and the opening signal releases this latch to open the circuit breaker by using the energy stored in the opening spring. The closing spring is usually recharged immediately after the closing operation. Closing spring is of higher energy level than the opening spring because it has to charge the opening spring as well as close the connection. Starting from the closed position with the charged closing spring, the breaker can complete O-C-O operation (open - close - open) without being recharged by the motor. Dampers are used to absorb excess energy at the end of stroke

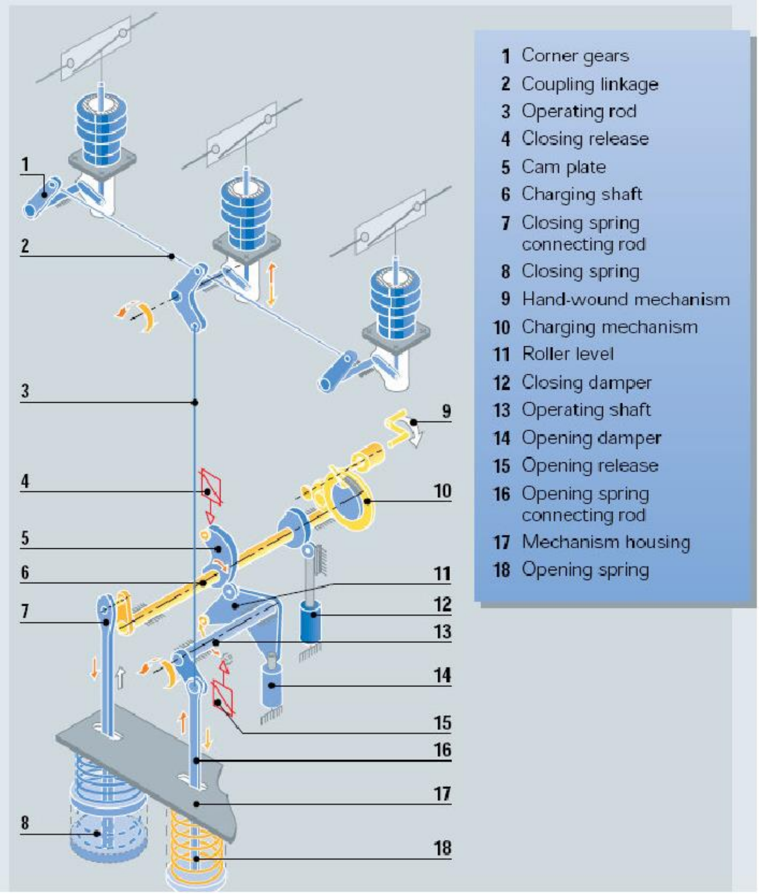

Figure 7: Spring operated Mechanism

Advantages:

a. Reliability of the spring mechanism can be improved with low energy operations.

b. There is no risk of leakage of oil or gas.

c. Less sensitive to variations in temperature than pneumatic or hydraulic mechanisms.

Limitations:

a. Tendency of impact operations during closing

b. Force output from a spring decreases along its stroke such that at the point of contact near the end of stroke, where the force requirements are maximum; spring force has fallen considerably.

c. Manufacturing of springs is difficult & costly.

d. Only one close open operation is possible by stored energy

It is observed from figure 8, that Closing time variation increases drastically with Hydraulic Mechanism for higher idle periods of the order 100hrs. Spring mechanism has shown quite consistent performance

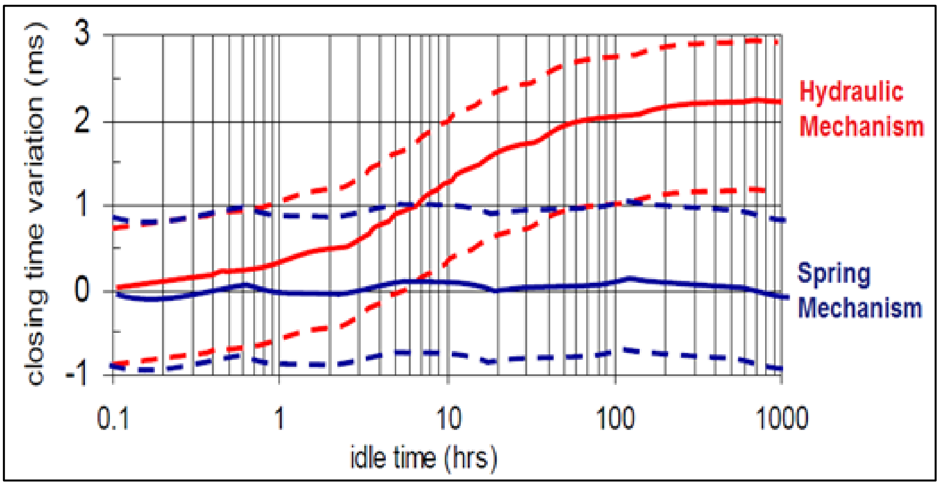

Figure 8: Comparison of spring and hydraulic mechanism

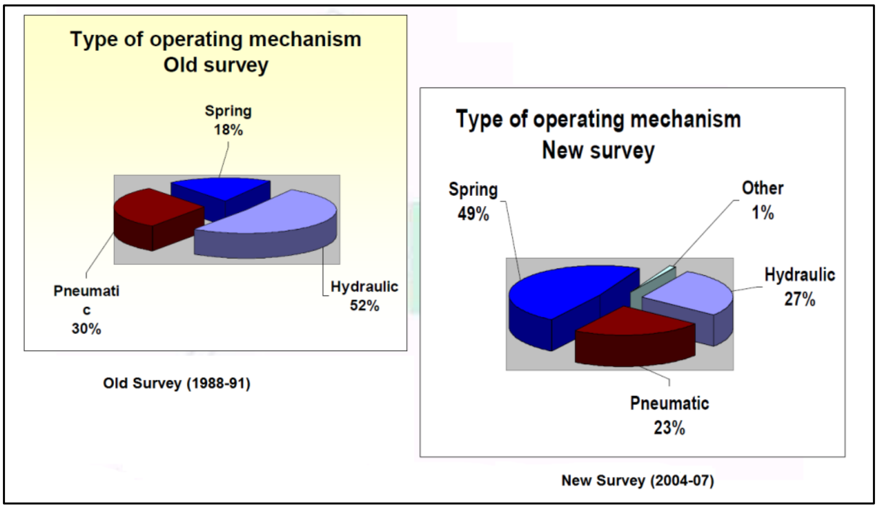

Figure 9: Mechanism population data

Mechanism population data is shown in figure 9. CIGRE results of survey for failure of breakers is shown in figure 10. Hydraulic mechanism is worst having highest failure rates. Below 200kV Spring mechanism failures are least. For GCBs above 200kV pneumatic mechanisms have shown better performance

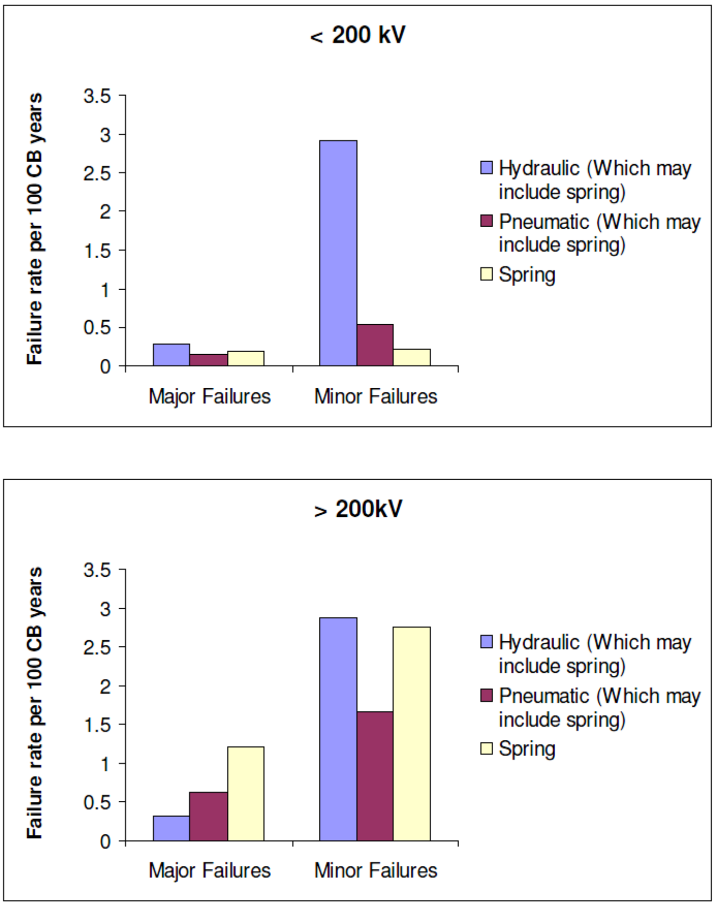

Figure 10: Failure data for mechanism

Heinemann [ ] concluded that the results obtained reveal that operating mechanisms with storage of energy in springs and energy transfer with a pure mechanical linkage or with a fluid seems to be most favorable for the future.

1.3.3. SUPPORT INSULATOR

The main function of the support insulator is to ensure sufficient insulation from the HV-terminals and the interrupter to the ground. The support insulator is a hollow housing made of porcelain or composite material and contains SF6 gas at the same pressure as that of SF6 gas in the interrupter. As we know that, interrupter is connected to high voltage line where high amount of current either flows or is interrupted. To prevent the flow of current from interrupter to the mechanism side (ground), an insulating rod called as pull rod is used which is connected between the operating mechanism and interrupter. This insulating pull rod which is a part of the linkage system between the operating mechanism and the interrupter is mounted inside the support insulator

1.3.4. SUPPORT STRUCTURE

To support the entire assembly of circuit breaker, a rigid structure is required which are made up of hot-dip galvanized steel.

1.4. THE DISPLACEMENT CURVE

Timing for closing and opening operation plays a critical in the design of circuit breaker. This puts great demands on the mechanical performance of all components in the interrupter chamber as well as the operating mechanism.

Two parameter; Instantaneous position (displacement) of the moving contact and instantaneous time are recorded for the complete operation and then plotted in the form of curve called as Displacement curve or Pole travel curve

Figure 11 shows displacement curve/pole travel curve for an opening operation.

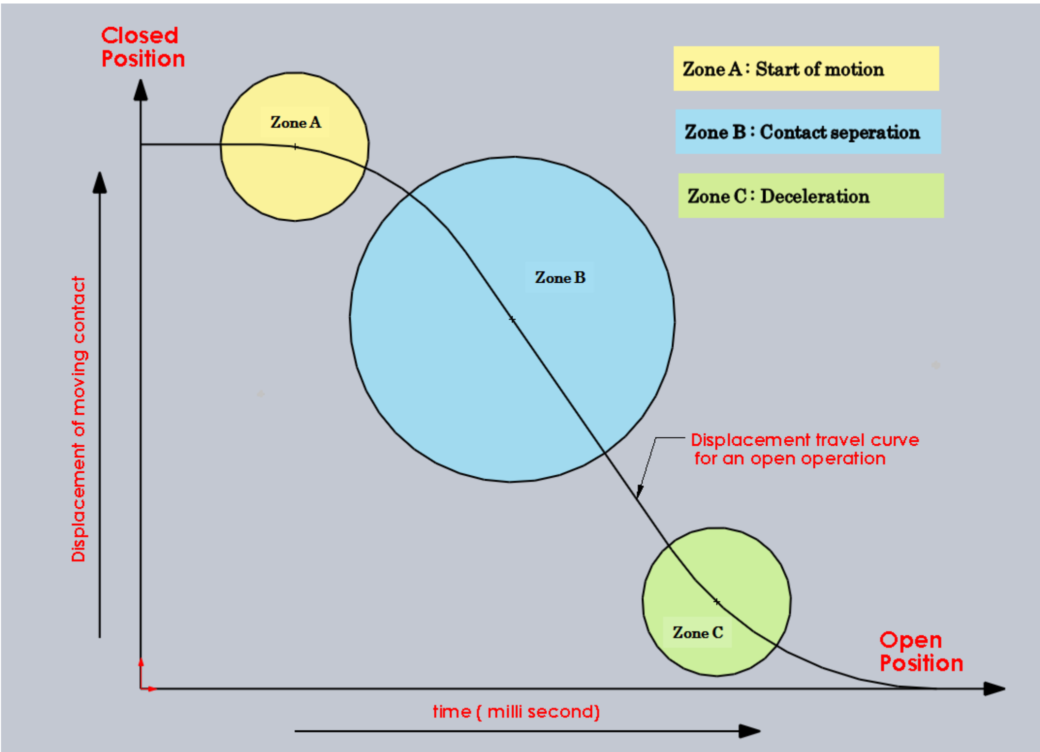

Figure 11: Displacement Travel curve for Opening Operation

In the above displacement curve, three zones have been marked.

Zone A: The Beginning of the Movement

This is where the movement starts. The Moving contact just starts separating itself from the fixed contact. It is extremely important to know whether the movement has begun at the right moment or not. For example, a delay with respect to the reference specification might be because of electrical problem where coil is not excited on time or it might be because of mechanical problem where a mechanical fault may exist between the command mechanism where the movement is triggered and the mobile contact of the breaker itself.

Zone B: Contact Separation

This is where the arcing contacts get separated from each other. At this instant, the arc begins to form and the high pressurized SF6 gas enters into the nozzle in order to extinguish the arc. The separation speed becomes an important factor in order to succeed in breaking the circuit. The method for calculating the average velocity in this zone depends on the breaker designer. Only the designer may determine the calculation method and establish the reference specification.

Zone C: Deceleration

This is where the movement decelerates until the circuit breakers moving contact comes to a complete stop. The amount of energy required in the separation of contacts depends upon voltage rating. Once the current has been interrupted and the arc has been extinguished, the energy developed is quite excessive. Effective means of damping are put into action to absorb this excess energy and thus reduce the risk of damaging the internal components of the circuit breaker. The analysis of this zone makes it possible to determine if the damping is optimal, which means the movement is stopped gradually. Insufficient damping, or under damping, allows the moving parts to undergo shocks at the end of the travel, which causes severe damage. A sudden damping, where the kinetic energy developed by the moving parts of the breaker is absorbed over very little time, causes damage similar to under damping. This phenomenon is called over damping.

1.5. TIME DEFINITION IN A CIRCUIT BREAKER

The plot between the displacement of the moving contact vs. time for the complete tripping operation has been referred as pole travel curve or displacement curve for opening operation.

Some of important time definitions that needs to taken into consideration while designing a circuit breaker are shown in figure 12.

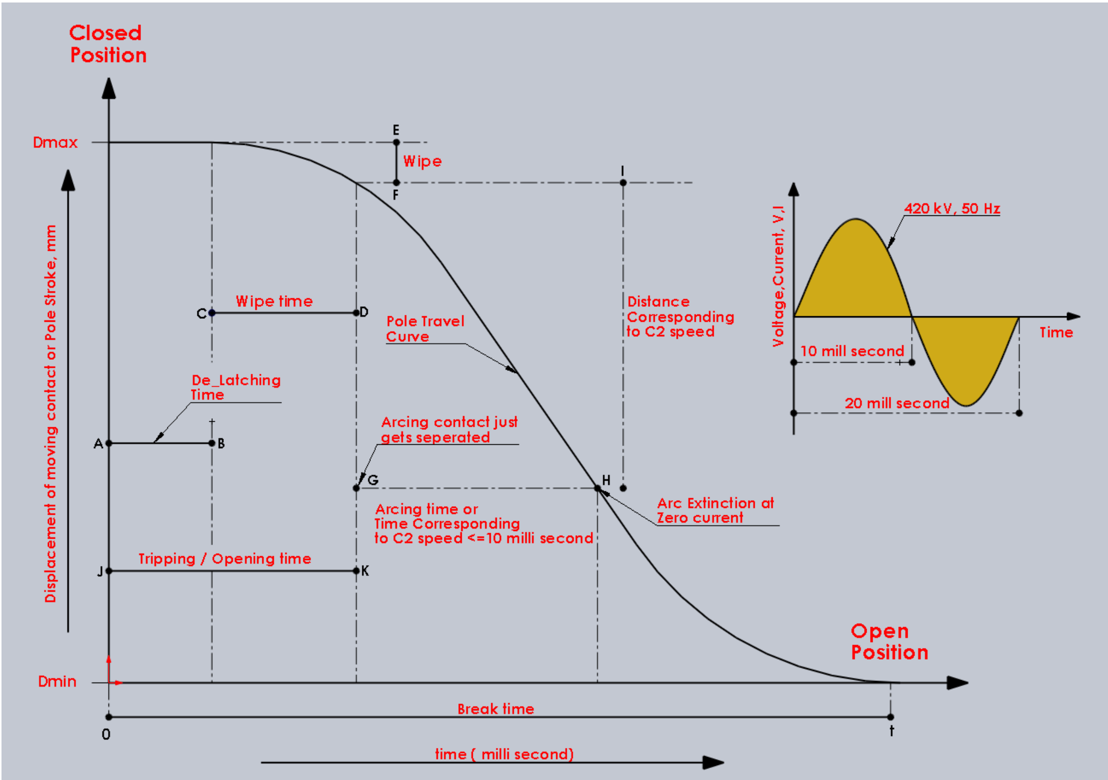

Figure 12: Time Definition on a displacement curve

a. De-Latching Time

Latch is a component in a circuit breaker that is used to hold the circuit breaker in its closed or open position. There are two Latches in a circuit breaker as shown in figure 13 below. First one is used for holding the circuit breaker in closed position and is called close holding latch while other Latch is used for holding the circuit breaker in open position and is called Trip holding latch. In most common arrangement, the closing spring is mechanically charged by motor and is held in the charged position by a latch. When the closing signal releases this latch, the spring drives the breaker to close and in the same motion it charges the trip spring. Another Latch holds the breaker in the closed position and the opening signal releases this latch to open the circuit breaker by using the energy stored in the tripping spring. Figure 13 shows general arrangement of Latch.

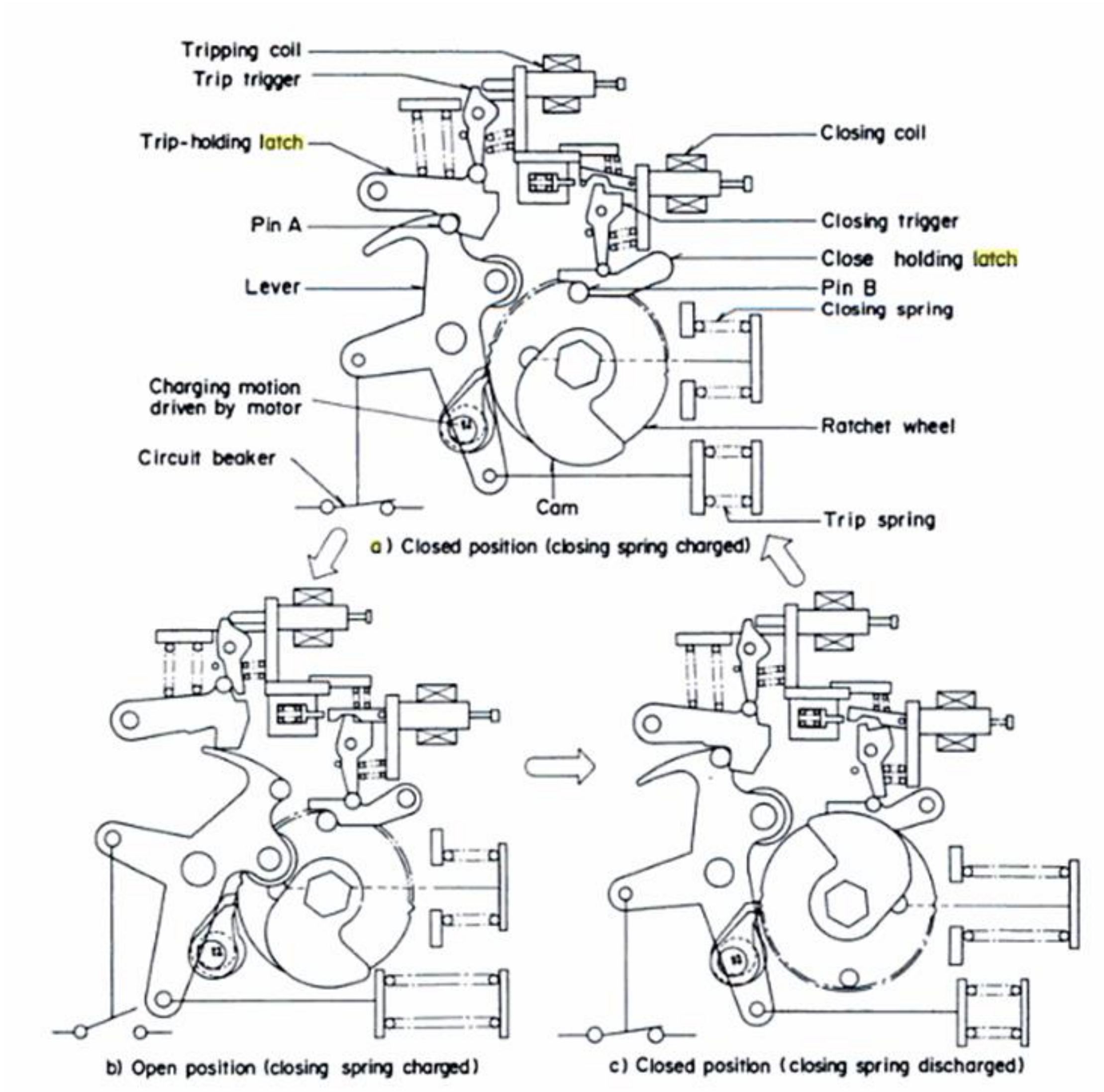

Figure 13: Latch arrangement in a spring operated mechanism

*De-Latching time for opening operation is the time interval between the instant the opening signal is given to the tripping coil to the instant when the Trip holding Latch just starts releasing or moving from its current position (closed position of circuit breaker).*Refer figure 12

b. Wipe Time

It is the time interval between the instant when trip holding latch is just released from its current position (connection closed) to the instant when the moving arcing contact just gets separated is called wipe time. The corresponding displacement of the moving arcing contact during this time interval is called wipe. Figure 14 shows the position of the moving arcing contact when the connection is completely closed and open. During tripping or opening operation, moving arcing contact starts moving relative to fixed arcing contact and when moving arcing contacts moves from point A to point B, contacts just gets separated. Displacement AB is called wipe and the time corresponding to this displacement is called wipe time.

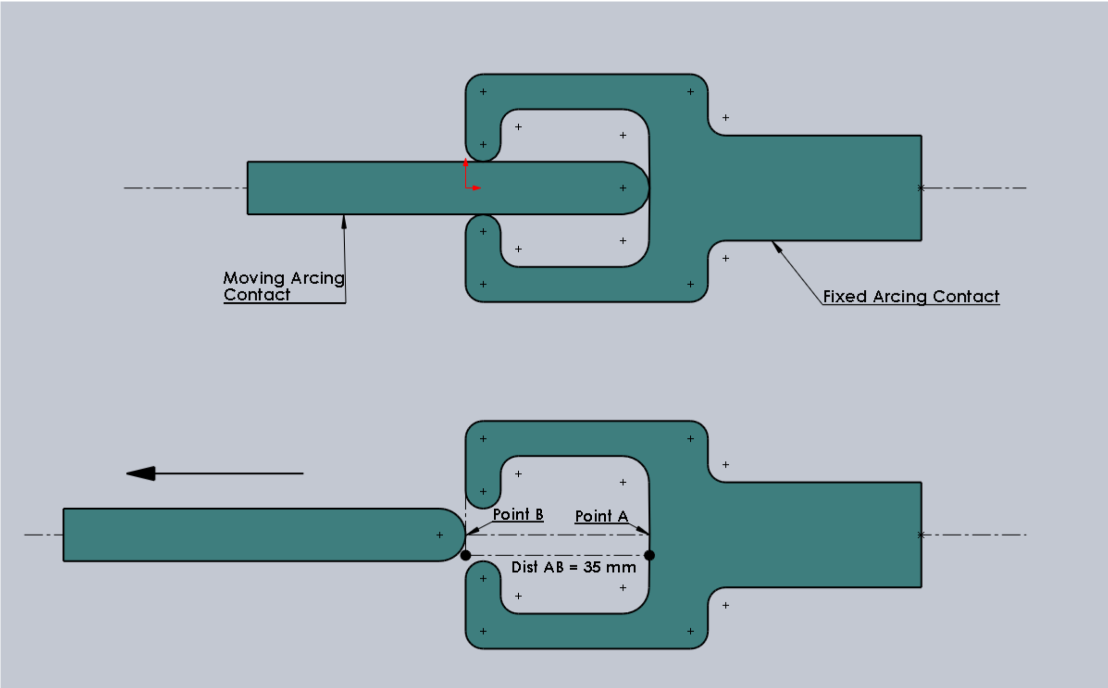

Figure 14: Opening of Contacts

In the current Design, the displacement AB (Wipe) is 35 mm so therefore Wipe time can also be defined as time corresponding to pole travel displacement of 35 mm. Refer figure 12.

c. Tripping Time or Opening Time

The time interval from the instant when the opening signal is given to the tripping coil to the instant when the arcing contact just gets separated is called tripping time or opening time. Refer figure 12. It is expressed as

$$Tripping\ time = De\_Latching\ time + Wipe\ time$$

d. Arcing Time

Once the arcing contact just gets separated relative to fixed contact, the medium between the two contacts gets ionized and glows in the form of arc. Arc produced in between the contacts needs to be extinguished as quickly as possible. In an AC power supply, Current zero or zero point is a very important aspect to arc extinguishing. Arc is extinguished naturally at every current zero but after crossing every current zero, the media between separated contacts gets ionized again during next cycle of current and the arc in circuit breaker is reestablished. To make the interruption complete and successful, this re-ionization in between separated contacts must be prevented after a current zero. The current is said to be "Current Zero" when the sine curve is at 0°, 180° and 360°. Arcing time is defined as the *Time span between the instant when the arcing contact just gets separated and there is first initiation of arc to the instant when the arc gets extinguished at current zero.* For 50 hertz, half cycle is executed in 10 millisecond and the value of current reaches zero again hence Arcing time will always be less than or equal to 10 millisecond. Refer figure 12.

e. C2 Speed

As we know that, In an AC cycle arc is extinguished naturally at current zero and is reestablished again after crossing current zero. To make the interruption complete and successful so that no re-ionization in between separated contacts takes place after current zero, moving arcing contact is made to move at a higher speed in Zone B so that stretching of arc occurs in between the contacts and sufficient SF6 is available to quench the stretched arc.

C2 speed is thus defined as the average speed with which moving arcing contact moves during arcing time.

$$C2\ speed = \frac{Distance\ travelled\ by\ moving\ arcing\ contact}{Arcinime}$$

f. Break time

Break time is defined as the time for complete separation of contacts. It is generally expressed in millisecond or cycles.

20 ms = 1 cycle at 50 hertz

CHAPTER 2

LITERATURE SURVEY

2.1. INTRODUCTION

Circuit breaker is one of the most important safety mechanisms. A comprehensive review of literature on the diverse aspects of circuit breaker is presented air. It helps to identify the area to be explored for further studies. Need for further research is explored.

2.2. CATEGORIZATION OF LITERATURE REVIEW

The review of literature has been divided in the following categories

a. Modeling and analysis of a circuit breaker mechanism, optimization of linkage system.
b. Modeling of friction in joints
c. Effect of Anelasticity and flexibility in components

2.3. OPERATING MECHANISMS FOR CIRCUIT BREAKER

Chen [1] derived the dynamic response equation of a spring-type operating circuit breaker in open operation by using the equation of motion. Equation of motion is a second order non linear differential equation given as

$$I(\theta)\,\ddot{\theta}\,(t) + C(\theta)\dot{\theta}^2(t) = M(\theta)$$

Where θ is the angular displacement of the input link, $I(\theta)$ is the generalized inertia, $C(\theta) = (1/2)(d[I(\theta)] / d\theta)$, and $M(\theta)$ is the generalized moment.

Based on definition of equation of motion, the kinematic coefficient of each machine member and its centre of gravity are derived to obtain the coefficients of the equation of motion. The equation is then solved numerically using the fourth order Runge – Kutta method and compared with experimental results. The analytical results revealed that the breaking time of the circuit breaker was 0.078 s, a mere 5% difference from the experimental result. Once the dynamic response of the circuit breaker is known, the input driving torque can also be computed from the equation of motion.

Cshoi [2] used multi body dynamics technique for optimizing the operating performance of a gas insulated circuit breaker. The circuit breaker consisted of several Latches and Cam as shown in figure 15.

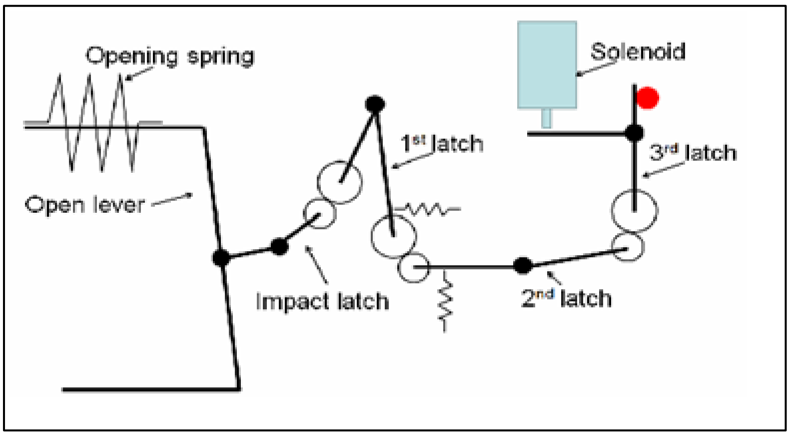

Figure 15: Operating mechanism of a circuit breaker

Figure 16 shows direction of latch motion and contact forces.

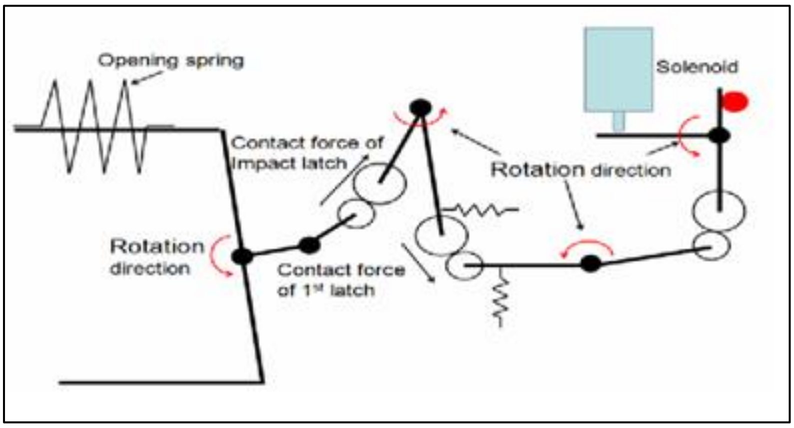

Figure 16: Direction of Latch motion and contact forces

The commercial software package Adams was used for the modeling and simulation of the circuit breaker. Each part of the breaker was considered as a rigid body in this study. Plunger Force and friction force data were given as input and corresponding angular displacement of first, second and third latch were obtained as results for simulation. These simulated results were further verified by comparing it with experimental results. A sensitivity analysis was then performed to determine the major variables that affected the performance of the system. The major variables identified using sensitivity analysis were

a. Spring length of second and third latch
b. Center position of the second latch roller.

These sensitivity analysis results were then verified using experiments and the simulation results from sensitivity analysis were in good agreement with the experimental data. From sensitivity analysis we could obtain upper and lower bound values of the major design variable which will result in the minimum opening time. The optimal design was then tested using Adams and Visual-DOC. The objective function was chosen to minimize the opening time during the opening process of the circuit breaker. The bound limits of the design variable were specified. The optimal values of design variables were obtained and correspondingly based on the simulation; the opening time of the circuit breaker was reduced by 1.5 milli second.

Jusng [3] defined a systematic procedure that optimized the performance of a gas circuit breaker using design of experiment. A multibody dynamic simulation model of the GCB was created. The first goal of optimization was to reduce the operating energy of the breaker from 4kJ to 2 kJ by improving the energy efficiency and the second goal was to reduce the volume of the system and increase the applying velocity. To achieve the two objectives above, two parts are optimized. First, the profile of a cam connected with a swinging crank and second is the position of the chains' pivot points, which transfers a spring force to the cam. Figure 17 shows concept diagram for GCB

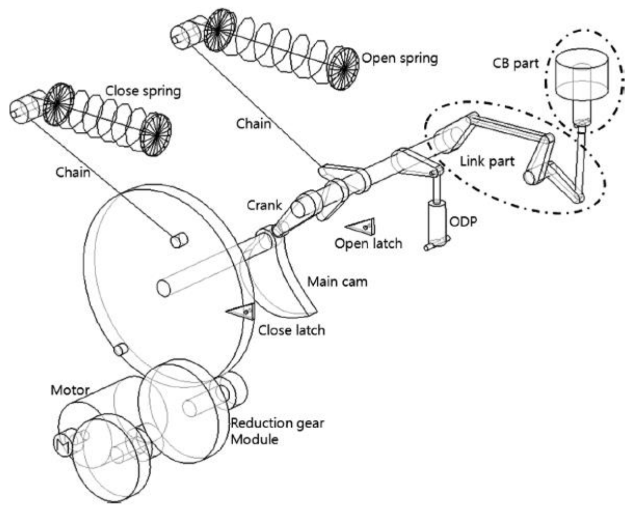

Figure 17: Concept diagram of a gas circuit breaker

A cam profile synthesis program was developed using MATLAB. An optimization module was inserted into this program and then the cam profile design and optimization were conducted simultaneously. The average pressure angle was chosen as the characteristic value to be optimized and decreased about 17.9% after the optimization. Using the multibody simulation model with the optimized cam system, the coordinates of the pivot points of the chains were optimized. After optimization, the average contact force was increased by approximately 13.95%. The optimized simulation model was capable of being operated with just 2 kJ, merely half of the energy originally required, and the applying velocity was increased. In addition, the volume of the whole system was reduced by 4.6%. Therefore, the required optimization objectives were all satisfied. Finally, the test result of the prototype of the breaker was nearly identical to that of the simulation result.

2.4. MODELING OF FRICTION IN JOINTS

Bender [4] provided an insight into fundamentals of friction modeling. Figure 18 shows the basic friction configuration.

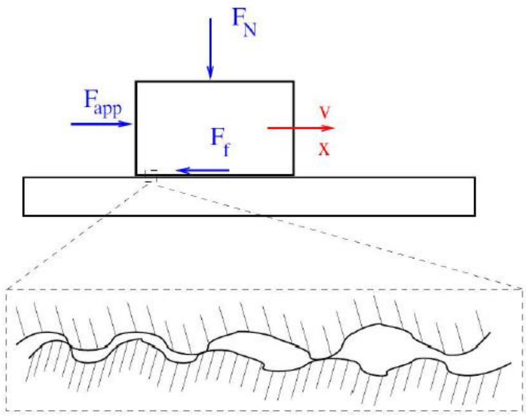

Figure 18: Basic friction configuration

Bender [4] explained that a close examination of sliding process reveals two friction regimes, Refer figure 19.

a. pre sliding regime
b. Gross sliding regime

Figure 19 shows two friction regimes and the transition from one regime to another.

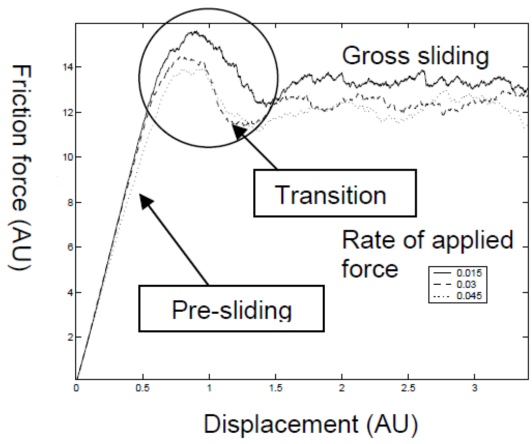

Figure 19: The two friction regimes and the transition between them

Pre sliding regime: In a pre sliding regime the adhesive forces, owing to asperity contacts, are dominant, and thus the friction force is primarily a function of displacement rather than velocity. Experiment reveals a hysteretic displacement dependent friction force.

Gross sliding regime: When the asperity junctions are continually being created and broken, the frictional interface is in the gross sliding regime. Frictional force is predominantly a function of velocity. Two main characteristics are of interest here

a. The Stribeck curve
b. Friction lag

Bender [4] proposed a generalized empirical friction model structure which takes into account all the above aspects of friction force. Most of the existing empirical friction models correspond to a generalized friction model structure, which consists in a friction force equation and a state equation. The friction force $\boldsymbol{F_f}$ is a generalized function of an internal state vector $\boldsymbol{z}$ (often representing asperity deflection), the velocity $\boldsymbol{v}$**,** and the position $\boldsymbol{x}$ of the moving object, that is

$$F_f = f(\boldsymbol{z}, \boldsymbol{v}, \boldsymbol{x})$$

The state equation that describes the dynamics of the internal state vector z is a first-order differential equation of the form

$$\frac{d\boldsymbol{z}}{dt} = g(\boldsymbol{z}, \boldsymbol{v}, \boldsymbol{x})$$

The functions f and g are generally nonlinear functions. In particular, it is shown that

$$f(\boldsymbol{z}, \boldsymbol{v}, \boldsymbol{x}) = f_1(\boldsymbol{z}, \boldsymbol{v}, \boldsymbol{x}) + f_2(\boldsymbol{v})$$

In the above equation, ***f1*** is responsible for the transient response in the velocity, while ***f2*** represents the instantaneous response to velocity changes.
Empirical friction modeling consists then in finding suitable expressions for the generalized functions ***f*** and ***g***, such that the resulting model faithfully simulates all observed types of friction behavior. Some of empirical friction model as stated are Dahl model, LuGre model, Leuven model, Generalized Maxwell slip model.

Fraczek [5] carried out a study on the unique solvability of a direct dynamics problem for mechanisms with redundant constraints and Coulomb friction in joints. It was observed that for a given rigid body mechanism the problem of finding joint reactions forces does not have a unique solution because of the presence of redundant constraint. If redundant constraints are present in the multibody system, the constraint equations are dependent and joint reaction forces could not be uniquely determined. If Coulomb friction in kinematic pairs is considered and reactions are non-unique, the simulated mechanism motion may not be unique as well. **Wojtyra [6]** stated that in the case of a redundantly constrained mechanism, despite the fact that all constraint reactions cannot be uniquely determined, selected single constraint reactions or selected groups of reactions can be specified uniquely. **Fraczek [5]** showed that — in general—the direct dynamic problem for an over constrained rigid body mechanism with Coulomb friction in joints is not solvable. This is a direct consequence of the fact that due to constraint dependency the normal joint reaction forces are not unique, and thus the friction (tangent) forces are not unique as well. However if friction forces appear only in these joints for which reaction solution is unique, then the simulated motion of mechanism is also unique, and thus — in this special case — the direct dynamic problem is solvable.

Muvengei [7] presented an effective approach of modeling and simulating the stick-slip friction in revolute clearance joints of a planar rigid multi body system. The

LuGre friction law is proposed to model the stick-slip friction by calculating the effective coefficient of friction (**μ**) as a function of relative tangential velocity of the contacting bodies and an internal state (***z***). The internal state ***(z)*** is considered to be the average bristle deflection of the contacting bodies that is the journal and the bearing of the revolute clearance joint. The normal force due to impact is modeled using **Lankarani and Nikravesh model [8]** which captures the energy dissipated during impact. **Muvengei [7]** obtained results from the simulation of a slider crank mechanism with revolute clearance joint in which stick slip friction was modeled using LuGre friction law. Figure 20 shows the slider acceleration and friction forces responses when the crank – connecting rod joint is modeled with 0.5 mm radial clearance. The input speed being $\mu_k = 0.1$ and $\mu_s = 0.2$.

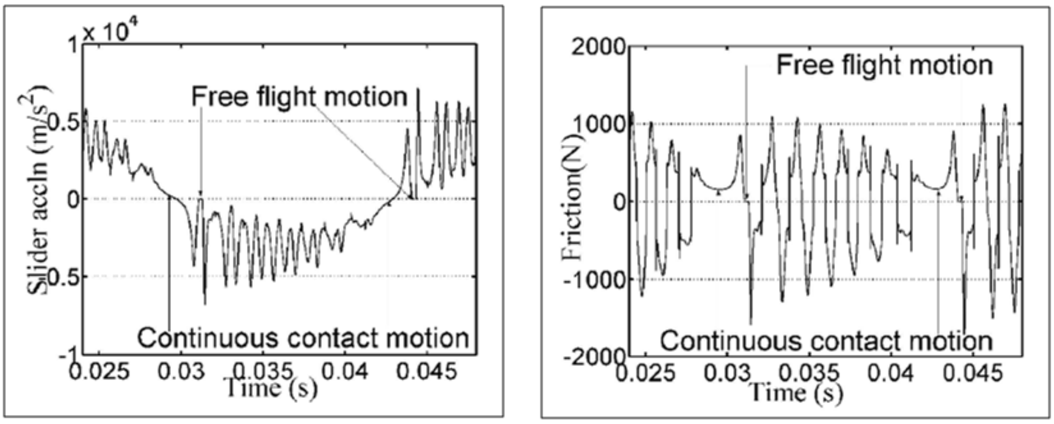

Figure 20: Slider acceleration and Friction force Response curve

When the journal moves freely inside the bearing walls; the slider moves with a constant velocity. This is replicated in the slider acceleration curve (figure 20) as regions of zero friction force since in free flight motion, no impact contact forces are created. The smooth regions in the slider acceleration curve indicate that the journal and bearing are in continuous contact motion. This situation is confirmed by the purely sliding friction in the friction force curve. The sudden change in the velocity of slider is due to impacts and rebounds between the journals and the bearing. These impacts are visible in the acceleration and the friction force curve as high peak values. Stick slip motion can be depicted from friction force curve. Hence the proposed representative version of LuGre friction law has been able to capture both the sliding and stiction friction together with stick slip motion inside a revolute clearance joint.

2.5. FLEXIBILITY IN MULTI BODY DYNAMICS

Zheng [9] analyzed the dynamic response of slider crank mechanism with clearance of the joints for a closed high speed press system. In this work, a traditional rigid model and a multibody rigid-flexible coupling dynamic model of the slider-crank mechanism with clearance of the joints in both the models was proposed using ADAMS software. In the rigid-flexible coupling model, the crank shaft and linkage were considered to be flexible elements. The clearance of the joints between the crank shaft and the main linkage, and between the main linkage and the main slider were taken into account for both the models. Figure 21 shows Slider crank mechanism with clearance joints.

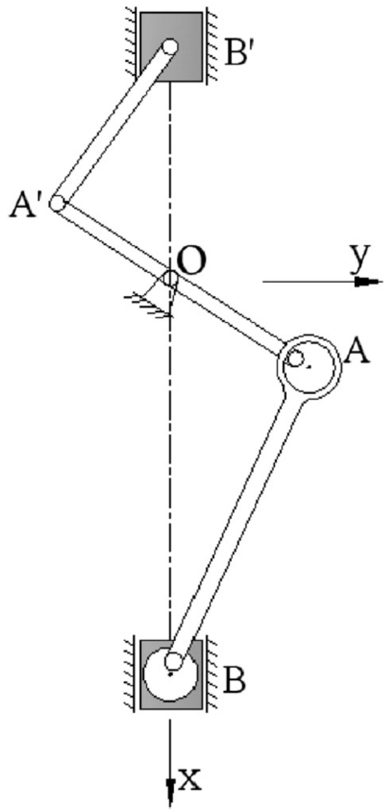

Fig. 2. The slider-crank mechanism with clearance joints.

Figure 21: The Slider - crank mechanism with clearance joints

The dynamic response of a mechanism with clearance was explored under the case of a mechanism with rigid crank shaft and linkage, and a case of a mechanism with flexible crank shaft and linkage. The simulation results showed that the dynamic response of the mechanism was influenced greatly by the clearance and the motion of the crank shaft center was characterized by three phases: a free flight motion, a contact motion and an impact motion with penetration

In the free flight motion, journal could move inside the bearing boundaries freely.

In the contact motion, journal and bearing were in permanent contact in a whole sliding motion.

In the impact mode that occurred at the end of the free flight mode, impact force were applied and removed in the system.

These 3 phases can be seen in the acceleration diagram for rigid model with clearance as shown in figure 22 and figure 20.

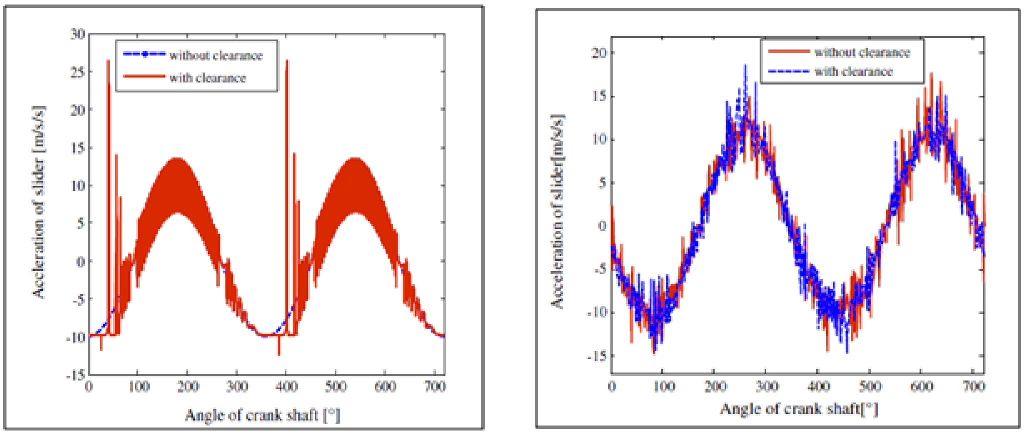

Figure 22: Acceleration diagram for rigid model (L) and rigid flexible model (R)

In the case of the flexible crank shaft and linkage, the maximum values of impacts and acceleration were highly reduced, and the elastic crank shaft and linkage acted as a suspension for the slider-crank mechanism. Figure 23 shows a journal center path of crank shaft for the traditional rigid model as well as rigid flexible coupling model of slider crank mechanism

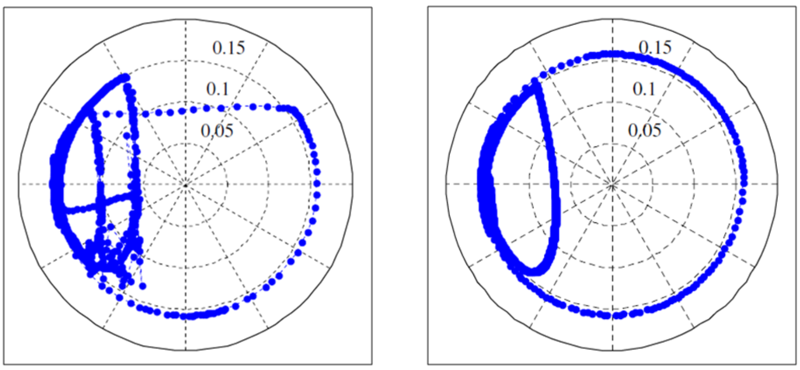

Figure 23: Journal center path of crank shaft for rigid model (L) and rigid flexible model (R)

From the above figure 23, we can conclude that with the introduction of flexibility, journal and bearing were in permanent contact for a very long time for the whole sliding motion and maximum values of impacts were reduced.

Classens [10] made a comparison between two breaker simulations, one with a stiff representation of linkages and other with an elastic representation, can be seen in Figure 24. As Visible in the figure 24, pole travel curves as well as axial force in the pull rod are plotted.

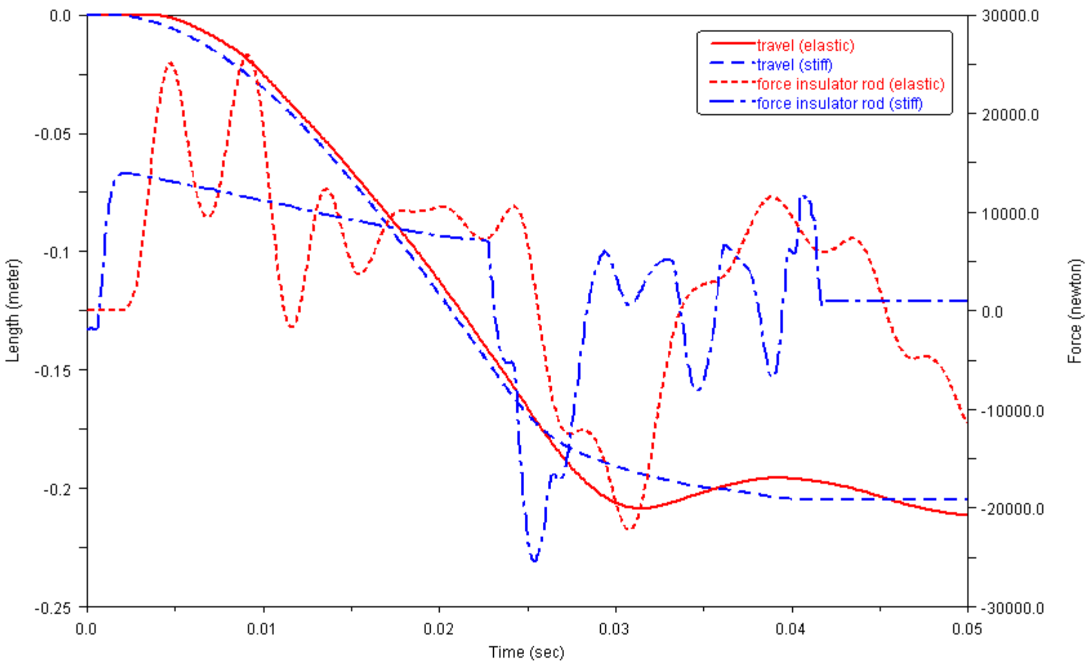

Figure 24: Comparison between stiff and elastic linkage

The maximal tensile force in the insulating rod differs by a factor of two between the both representations. It is evident that such a big difference may have a big impact on component design, hence a correct representation of the mechanical chain is essential to reduce the number of development tests and there by the development time.

2.6. CONCLUSION OF LITERATURE SURVEY

The literature related to circuit breaker has been discussed elaborately in the previous section. As apparent from the literature review, there has been immense research on the performance improvement of circuit breaker. Friction and flexibility has been taken into account by many researchers so as to model a multi body dynamics problem closer to reality. There is a vast scope of improvement in the performance of a circuit breaker where timing for operation can be further minimized.

CHAPTER 3
PROBLEM DEFINITION

The primary function of an electrical circuit breaker is to provide opening and closing the current carrying contacts. Circuit breaker must be able to perform its function reliably, without any delay or sluggishness. A slow or sluggish response of a circuit breaker will result in unnecessary disruptions to electricity supplies and maintaining high fault currents for extended durations can stress the network thus causing damage to plant and equipment.

Main design criteria for a circuit breaker are quick and timely disconnecting and reconnecting different parts of power system network for protection and control.

The first objective of this thesis is to improve the performance of a 420 kV gas insulated circuit breaker by minimizing the wipe time. There are many parameters that can have an influence on the wipe time. These parameters need to be identified and further studying their effect on the wipe time is a challenge.

Also as stated, pull rod link is connected between the operating mechanism and interrupter. The material for the pull rod is an insulating material and in the current study fiber reinforced plastics (FRP) is used. The only limitation with insulating material is that they exhibit large elastic deformation and hence behave as a flexible material. Flexibility in the pull rod may influence the wipe time and hence studying its effect is another challenge for us.

The second objective of this thesis is to study the effect of flexibility on the wipe time.

CHAPTER 4

DYNAMICS OF CIRCUIT BREAKER

4.1. MODELLING OF SIMPLIFIED MODEL FOR A CIRCUIT BREAKER

A standard multi body SOLID WORK model of a 420 kV circuit breaker and its Multi body dynamics (MBD) inputs && simulation results was given to us. A simplified multi body rigid model of the circuit breaker was then established in SOLID WORK with standard model as reference. All the links were considered as rigid links. Figure 25 shows the diagram of the simplified multi body model of a circuit breaker.

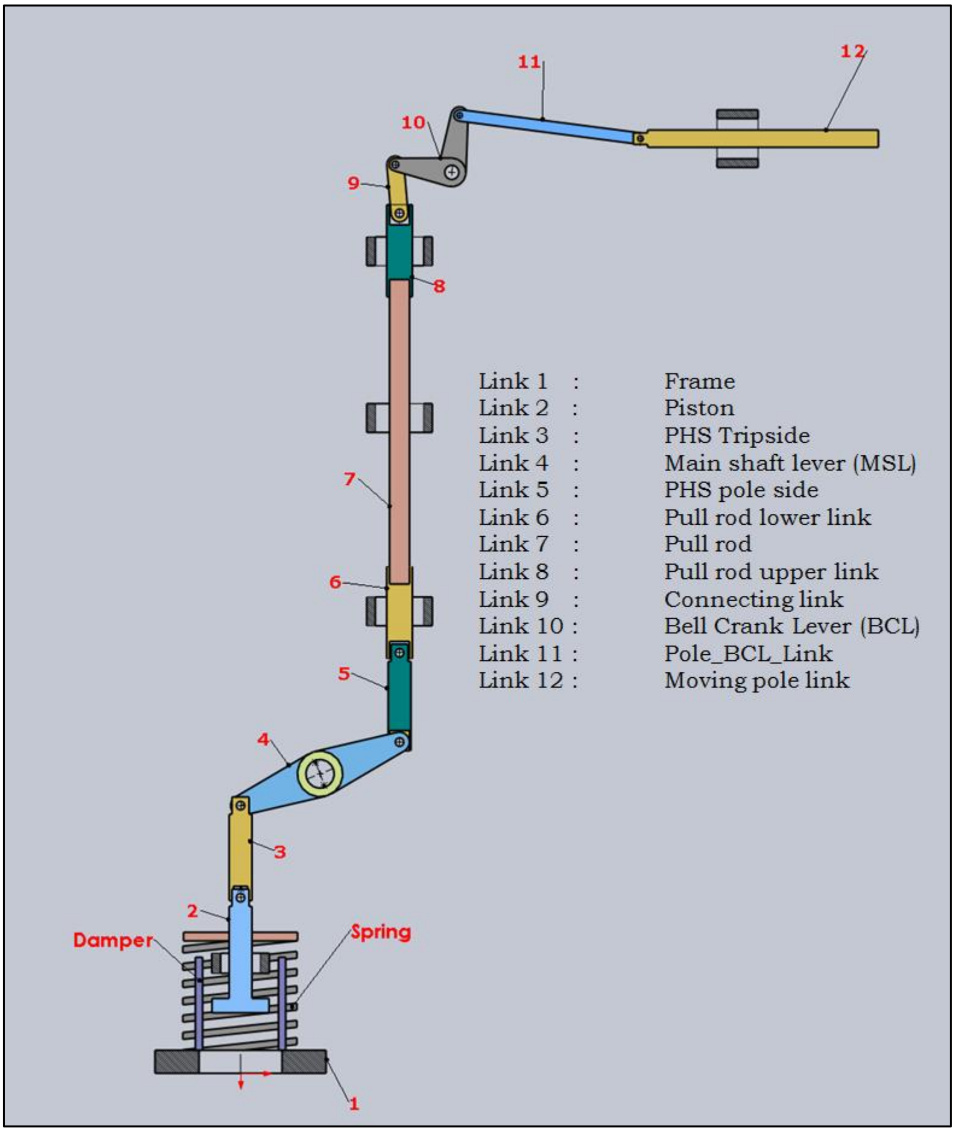

Figure 25: Simplified Multi body model for a circuit breaker

As seen from the figure 25, spring type operating mechanism was used for opening operation. Simplified multibody model differed from the standard multi body model in terms of complexity and consisted of few numbers of linkages. Masses of each link of the standard multi body model were recorded and then assigned to the simplified model. Effective mass calculations were done in order to reduce the number of linkages in the Standard model. An example for effective mass calculation is shown figure 26 and figure 27.

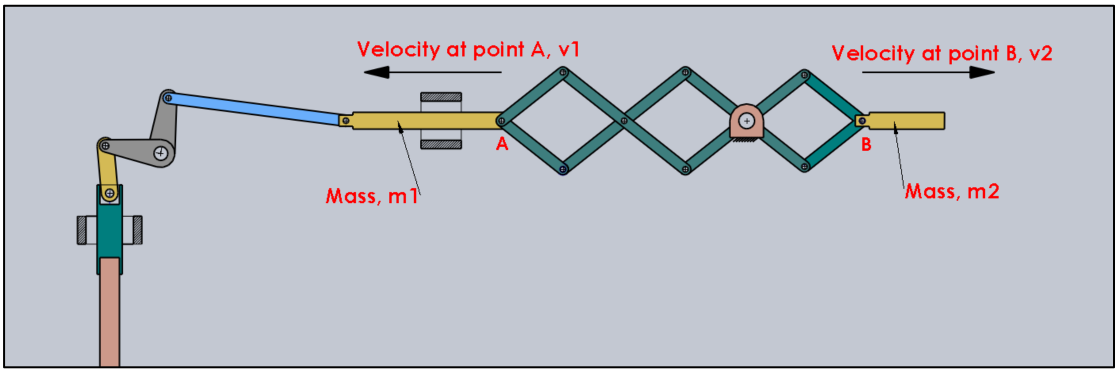

Figure 26: Portion of Standard Model

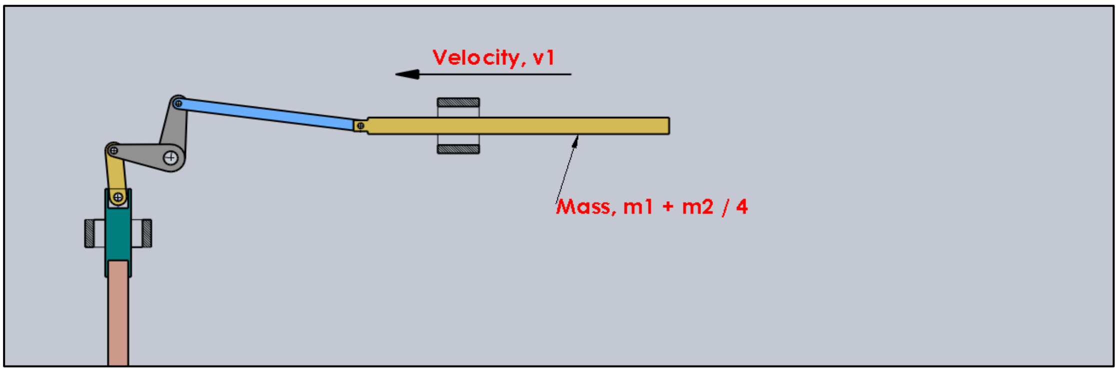

Figure 27: Portion of simplified model

Whenever a mass element is separated from another element by a lever ratio or a gear ratio, its effective value is modified by that ratio

As seen in figure 26,

Let

m1 and m2 be the masses of the respective link

v1 and *v2* are the velocities of the respective link at point A and B

In effective mass calculations, we need to calculate the effective mass that must be placed at point A in order to eliminate lever.

Since m1 and m2 masses are separated by a lever ratio, so we need to calculate equivalent mass that must be placed at point A in order to eliminate lever. Equating the kinetic energies in the masses at point A and point B

$$\frac{1}{2}\, m_2 v_2^2 \;=\; \frac{1}{2}\, m_{eff}\, v_1^2$$

Velocities at each end of the lever is related as

$$v_2 = \; v_1/2$$

Substituting the value of v_2 from Equation 2 into Equation 1, we get

$$m_{eff} = \; m_2/4$$

Total mass at Point A is given as

$$m_{tot} = \; m_1 + \; m_2/4$$

The advantage of simplified model over standard model was that the computation time required for performing MBD through SOLID WORK MOTION ANALYSIS was reduced significantly.

4.2. MBD OF A SIMPLIFIED MULTI BODY MODEL

Once a simplified model was established in SOLID WORK, its dynamic behavior was required so as to further study it response to the set of forces. MBD was performed on simplified model using SOLID WORK MOTION ANALYSIS.

4.2.1. INPUTS FOR MBD

The direction of motion and set of forces acting on the simplified model of the circuit breaker are shown in fig below. The set of forces acting on the circuit breaker were given as

a. Spring Force
b. Damping Force
c. Pole Force

d. Inertia Forces

Refer figure 28 for reference

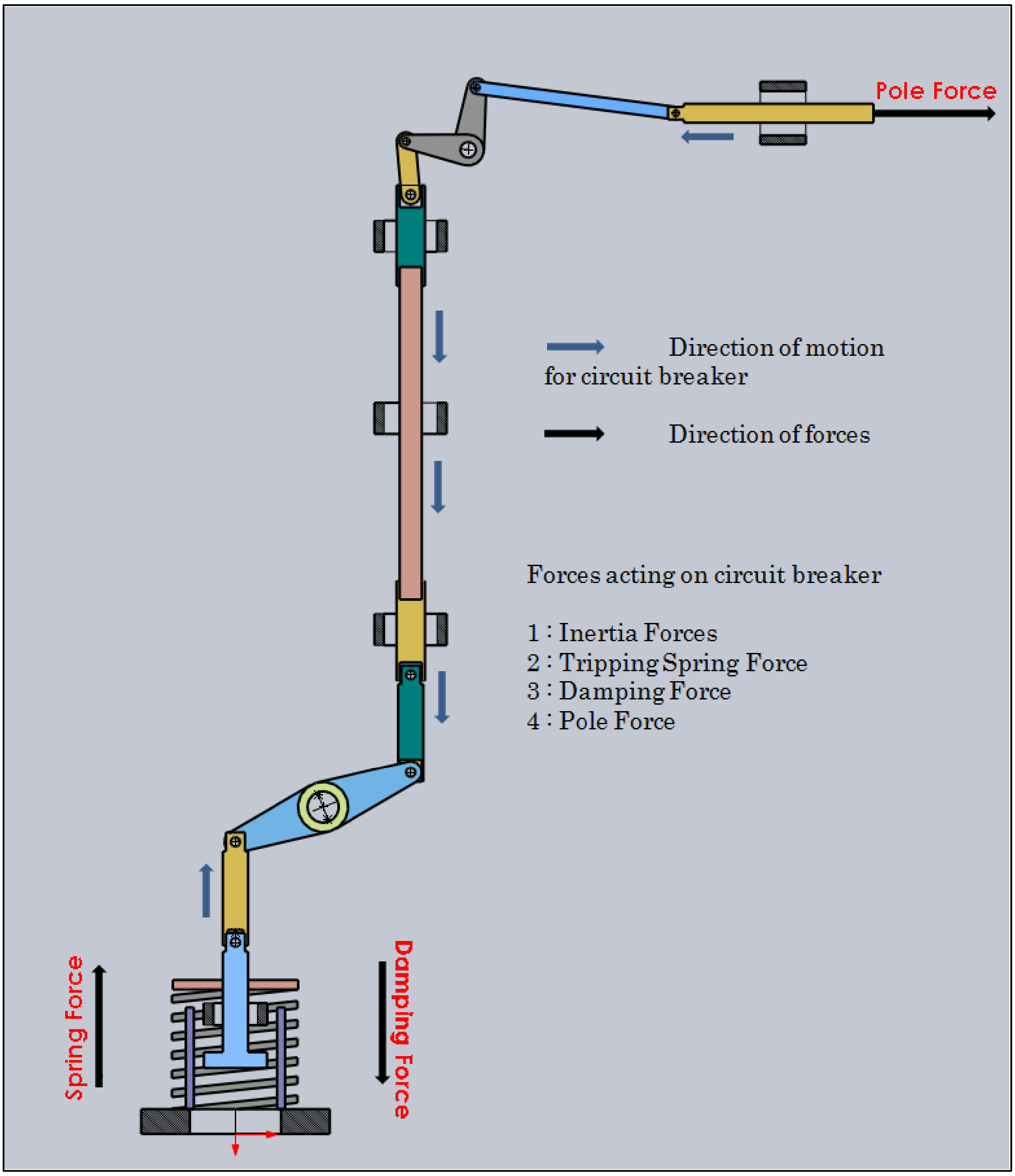

Figure 28: Forces in a circuit breaker

4.2.1.1. SPRING FORCE

There are two parameters that are required while defining a spring element in SOLID WORK MOTION ANALYSIS. They are stiffness of the spring and free length of the spring. The value of stiffness was considered same as defined in the case of standard multi body dynamic model. Calculation for the free length of the spring was made as follows. All the given parameters for free length of the spring calculation are given in table 2.

Given Parameters for free length of the spring calculation			
S. no	**Parameter Name**	**Units**	**Description**
1	Stiffness, k	N/mm	Same as defined in Standard model
2	Maximum Load by the compressed spring, $Fmax$	N	-
3	Initial Compressed Length of the Spring	mm	Given, Referred from simplified solid work model

Table 2: Given parameters

Figure 29 shows the state of the spring.

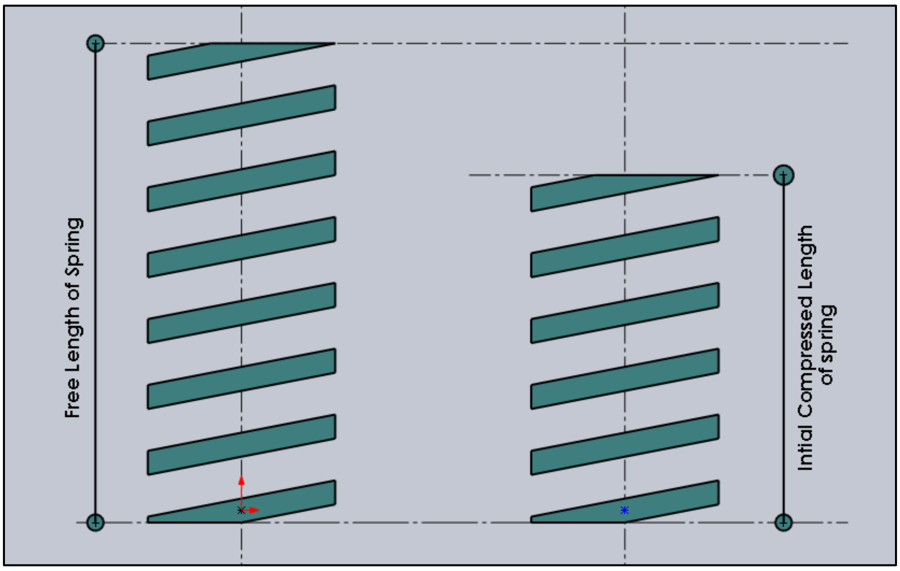

Figure 29: State of the spring for free length calculation

Free length of the spring was given as

$$Fmax = -kx$$

$$Fmax = -k(Initial\ compressed\ Length - Free\ Length)$$

$$Free\ Length = \frac{(Fmax + k\ \times Initial\ compressed\ Length)}{k}$$

4.2.1.2. DAMPING FORCE

Damping force for simplified model was considered same as defined in standard multi body dynamic model. Damping force was defined as function of velocity of piston and the displacement of piston. Figure 30 shows the plot of Damping Force versus time.

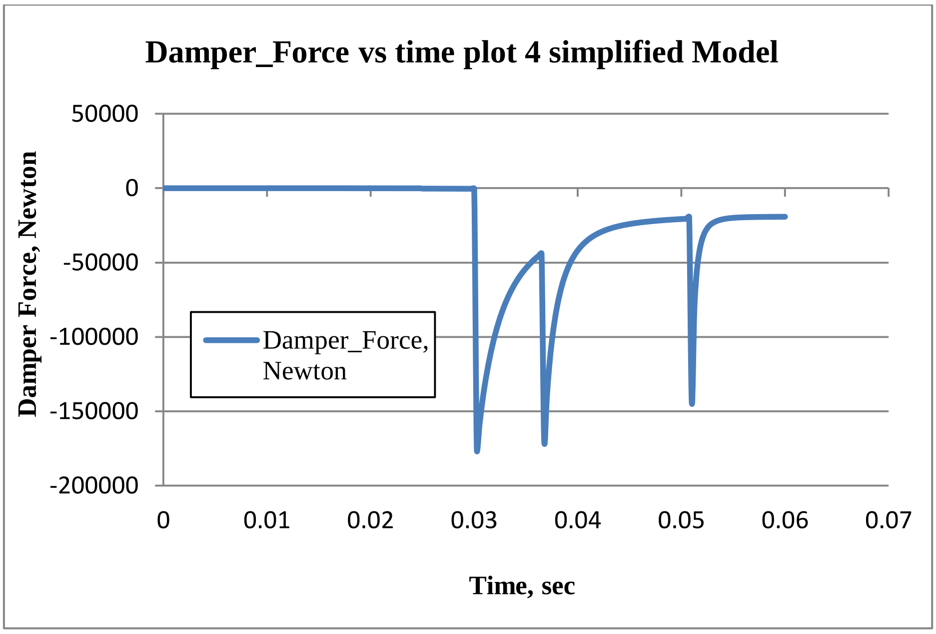

Figure 30: Damping force plot

The explanation for damping force being a function of velocity of the piston and displacement of piston is explained through damping for model. Figure 31 refers to the damping force model.

Let

P : pressure acting on the piston by the oil/fluid

A : Net X-Sectional area of the piston

a : X-sectional area of the opening/orifice

ρ : Density of oil/fluid

V : Velocity of Piston

v : velocity of fluid/oil flowing out of the opening/orifice

F : Damper force

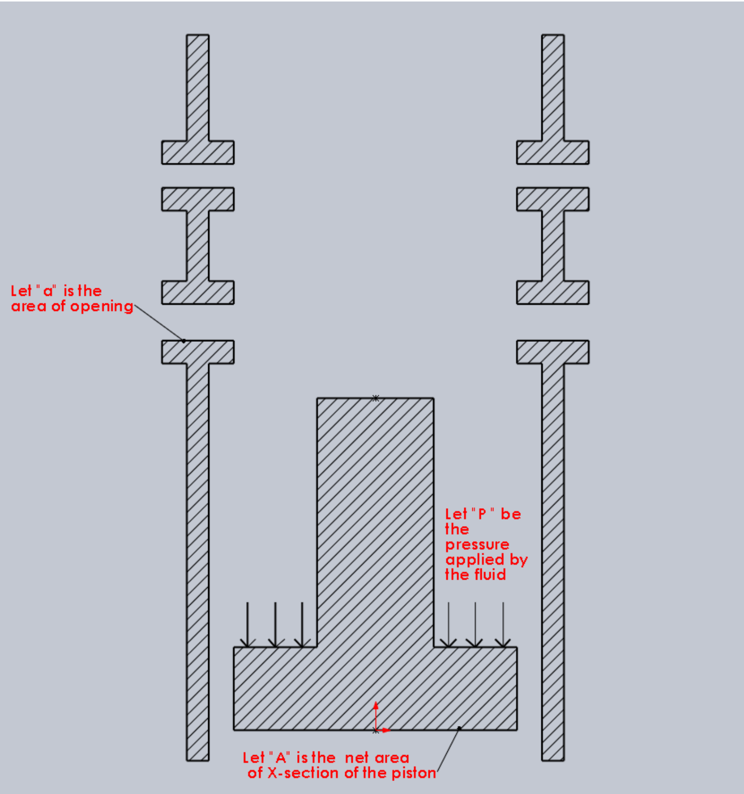

Figure 31: Damping force model

Damping force is given as

$$F = P \times A$$

Where Pressure P is calculated from Bernoulli's theorem as

$$P = \frac{\rho V^2 A^2}{2a^2}$$

Hence

$$F = Constant \frac{V^2}{a^2}$$

Since ***a***, X-sectional area of the opening changes with the displacement of the piston hence the above expression clearly reflects damping force being a function of velocity of piston and displacement of the piston.

4.2.1.3. POLE FORCE

As stated SF_6 gas is used for quenching of arc. During opening operation, SF6 gas gets compressed and exerts pressure on the cross-section of the moving cylinder. Pole force is thus defined as the force exerted by SF6 gas on the cross section of the moving cylinder. Refer Figure 32.

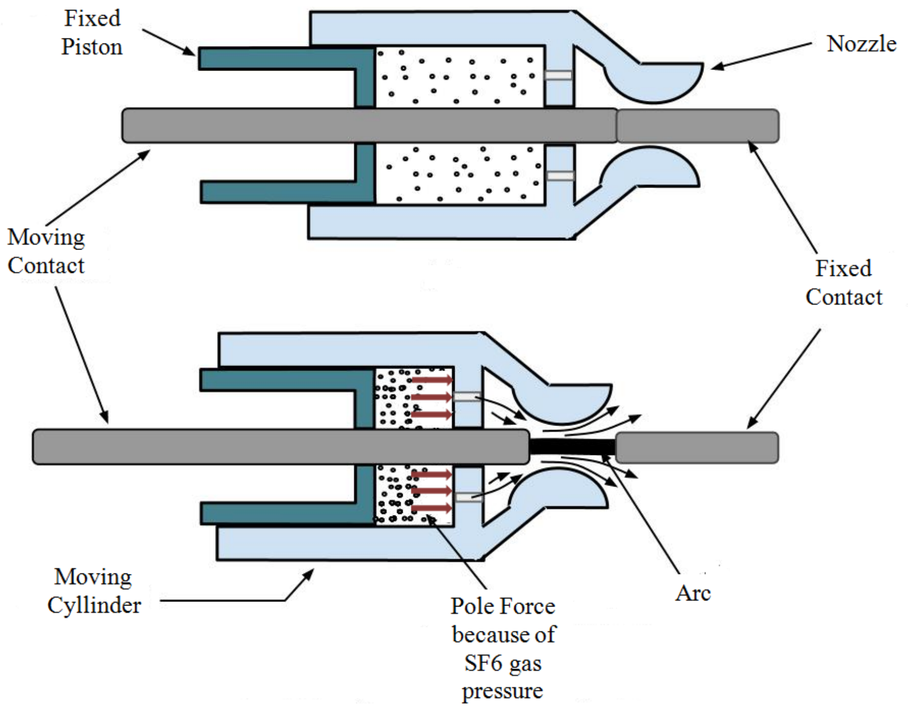

Figure 32: Pole Force

Pole force was considered same as defined in standard multi body dynamic model. Its value was assumed as constant.

4.2.2. RESULTS OF SIMPLIFIED MODEL

Once the inputs and constraints were defined for simplified model in SOLID WORK, GSTIFF integration method was used for Solid works motion solver.

Following were the results obtained after performing MBD.

a. Tripping spring force versus time plot

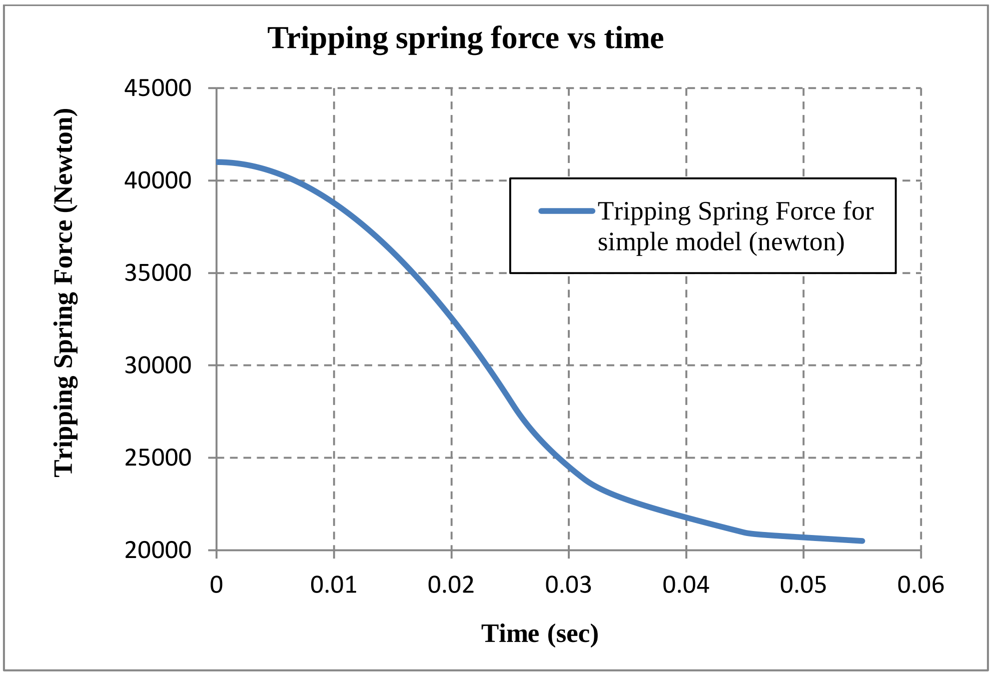

Figure 33: Tripping spring force plot

b. Velocity of piston versus time plot

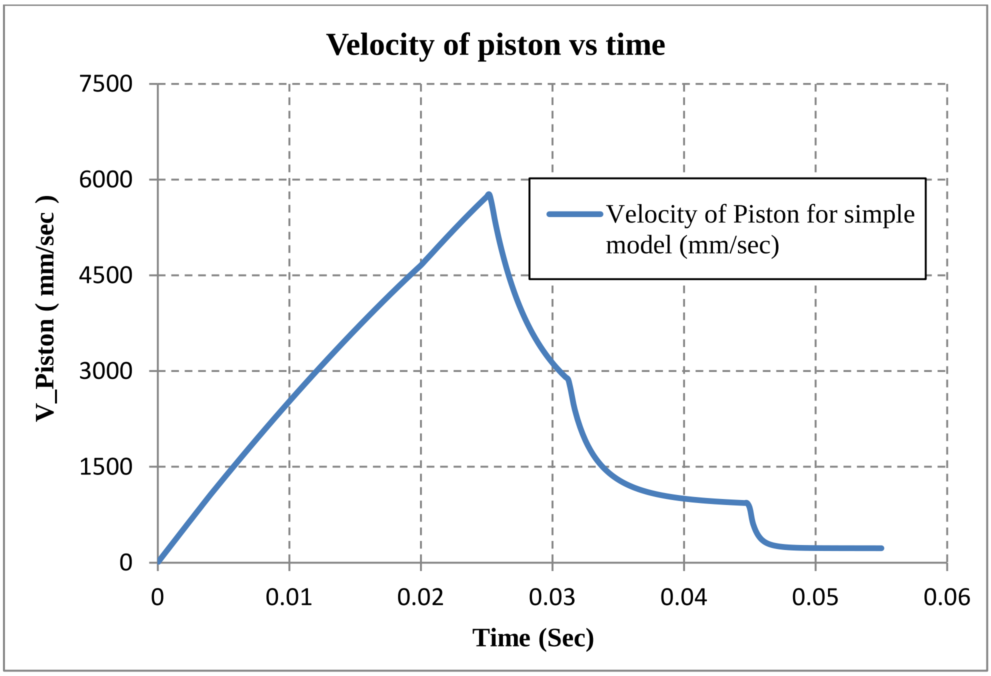

Figure 34: Velocity of piston plot

c. Displacement of piston versus time plot

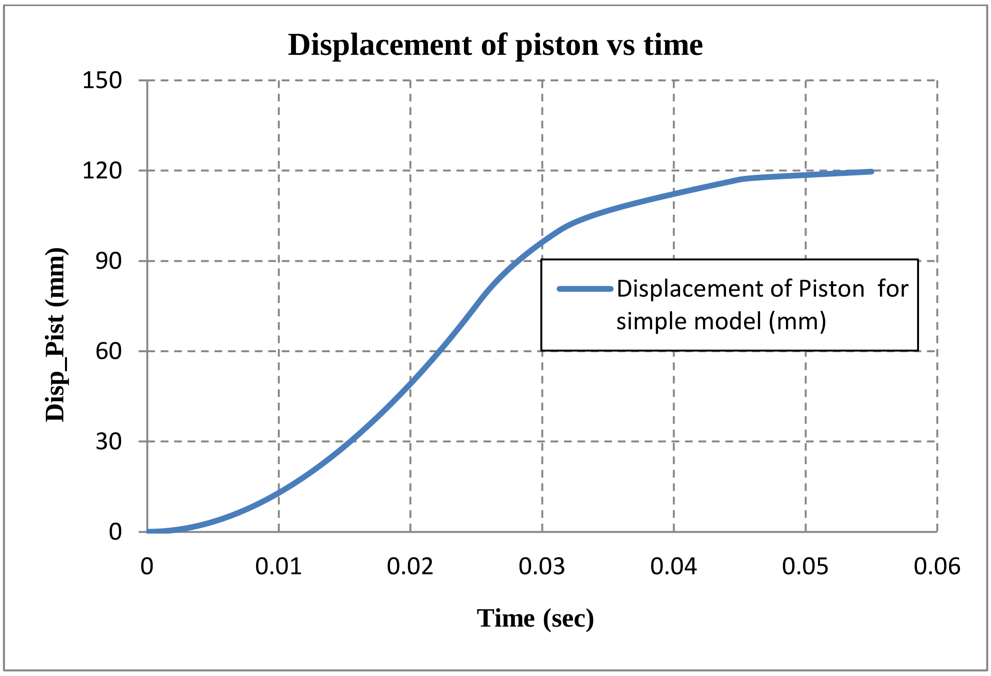

Figure 35: Displacement of piston plot

d. Pole travel versus time plot

Displacement of the pole moving link at any instant is called pole travel at that instant. The plot of pole travel vs time is called pole travel curve.

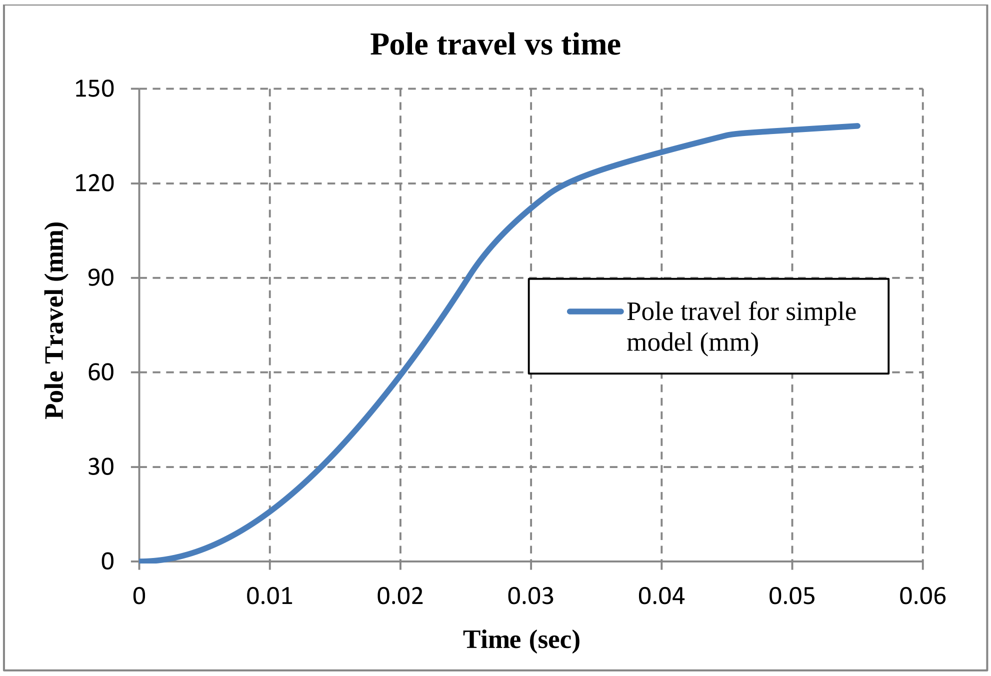

Figure 36: Pole travel plot

e. Angular displacement of main shaft lever versus time plot

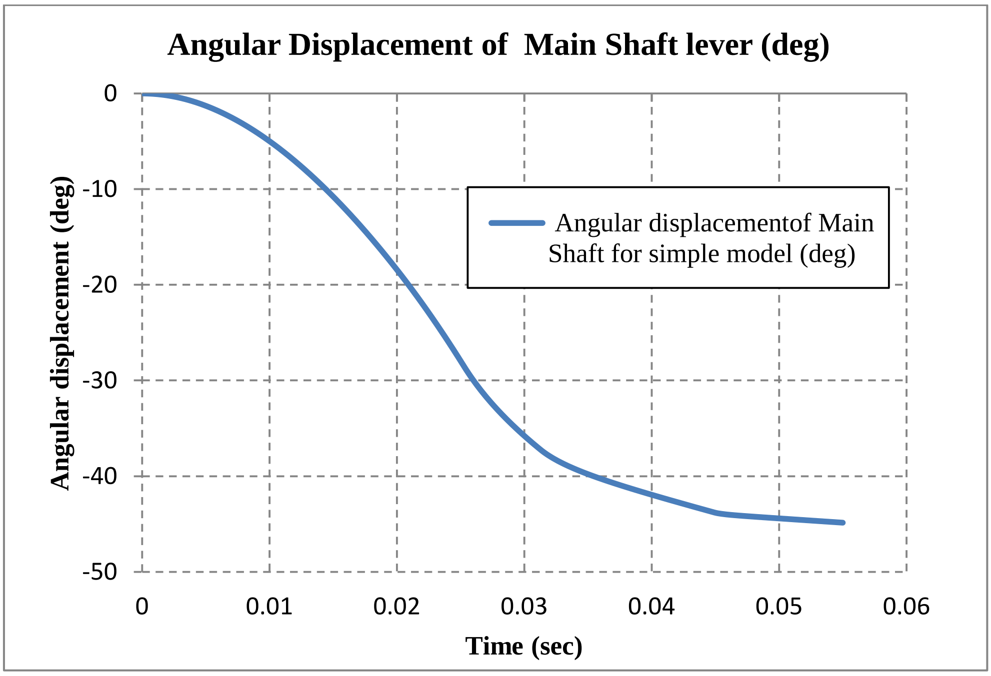

Figure 37: Angular displacement of MSL plot

f. Angular displacement of Bell crank lever versus time plot

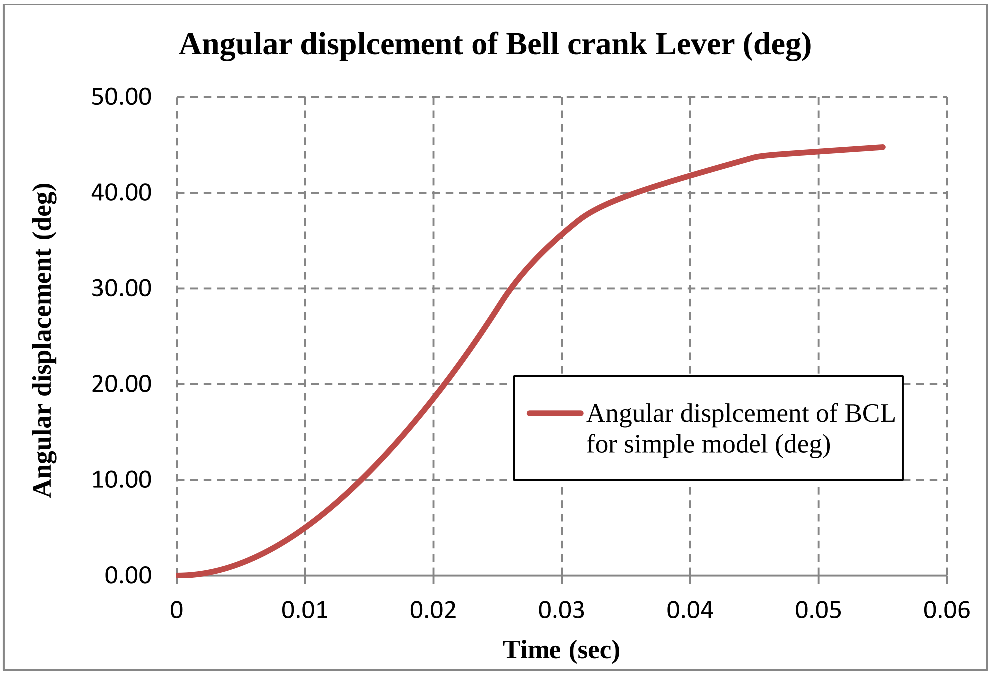

Figure 38: Angular displacement of BCL plot

4.3. COMPARISON OF SIMPLIFIED AND STANDARD MODEL SIMULATION RESULTS

Above MBD simulation results obtained for simplified model were then compared with the results available for standard model. Simulation results for simplified model were in good agreement with the results for standard model. Hence a simplified solid work model exactly replica of the standard model was now available to us. Wipe time obtained from pole travel curve (Refer Fig 36) was 15.2 milliseconds. Our next goal was to minimize this wipe time which is dealt in the next chapter.

CHAPTER 5

PARAMETRIC MODELLING AND ANALYSIS FOR WIPE TIME

5.1. INTRODUCTION

Simplified model of the circuit breaker analogous to the standard model was now available with us. Its MBD Simulation results were in good agreement with the results for the Standard model. Our next task was to identify the parameters that could influence the wipe time and further study their effects on wipe time.

5.2. IDENTIFICATION OF PARAMETERS

All the possible parameters that could influence the wipe time were identified and are presented below

a. Mass of the moving pole link
b. Mass of the pull rod
c. Stiffness of the spring
d. Linkage dimensions

5.3. EFFECT OF THE MASS OF THE MOVING POLE LINK

In the simplified model, mass of the moving pole link was varied in steps and for each change in mass; MBD was recalculated using SOLID WORK MOTION ANALYSIS. Rest of the parameters like stiffness, damping, pole force and masses of other component were kept same. Simulation results revealed that as the mass of the moving pole link decreased, there was a corresponding decrease in the wipe time. As the mass of the moving pole link reduced by 3 kg, 2.6 % reduction in wipe time was reported. Reason for this is explained as, with the same amount of spring Force, reduction in mass cause's higher acceleration and lower inertia forces. Thus wipe time decreases.

5.4. EFFECT OF THE MASS OF THE PULL ROD

Similar procedure as done for the above case was followed here. In this case, mass of the pull rod was varied in steps and for each change in mass, MBD was recalculated. Rest of the parameters was kept same. Simulation results revealed that, as the mass of the pull rod was reduced by 2 kg, there was a reduction of 1.3 % in the wipe time. Further reduction in mass of the pull rod by 2 kg had no affect on the wipe time.

5.5. EFFECT OF THE MASS OF THE PULL ROD AND MASS OF THE MOVING POLE LINK

Combining the above two cases, simulation results reported that when the mass of the pull rod and the moving pole link was reduced by 2 kg and 3kg, wipe time reduced by 3.9 %.

5.6. SUMMARY OF THE VARIATION IN MASSES ON THE WIPE TIME

Below Table 3 provides the summary of the effect of masses of the pull rod and moving pole link and their combination on the wipe time.

Case no	**Mass of the moving pole link, Kg**	**Mass of Pull rod, Kg**	**Wipe time, millisecond**
	Meff	**M_{IPR}**	**t**
1	16.9	16.6	15.2
2	13.9	16.6	14.8
3	16.9	14.6	15
4	16.9	12.6	15
5	13.9	14.6	14.6

Table 3: Summary of effect of masses on wipe time

5.7. EFFECT OF THE STIFFNESS OF THE SPRING

As stated, there are two parameters that are required while defining a spring element in SOLID WORK MOTION ANALYSIS.

a. Stiffness of the spring
b. Free Length of the spring

Values for the stiffness of the spring were increased in steps and corresponding free length of the spring was calculated keeping spring energy released and stroke same in all the cases. Hence our next step was to calculate spring energy released during opening operation for simplified model.

5.7.1. CALCULATION OF SPRING ENERGY RELEASED FOR SIMPLIFIED MODEL

Our next task was to calculate the spring energy released during opening operation for the simplified model. For a given simplified model, all the calculated and given spring parameters as stated in the previous chapter are defined in the following table 4

Given Parameters			
S.no	**Parameter name**	**Value**	**Units**
1	Stiffness, *k*	171.3	N/mm
2	Stroke	120	mm
3	Max Load by the spring, *Fmax*	41	kN
4	Initial compressed length	377	mm
5	Free Length	616.3	mm

Table 4: Given Spring parameters

Figure 39 shows the pictorial description of the state of the spring before and after opening operation.

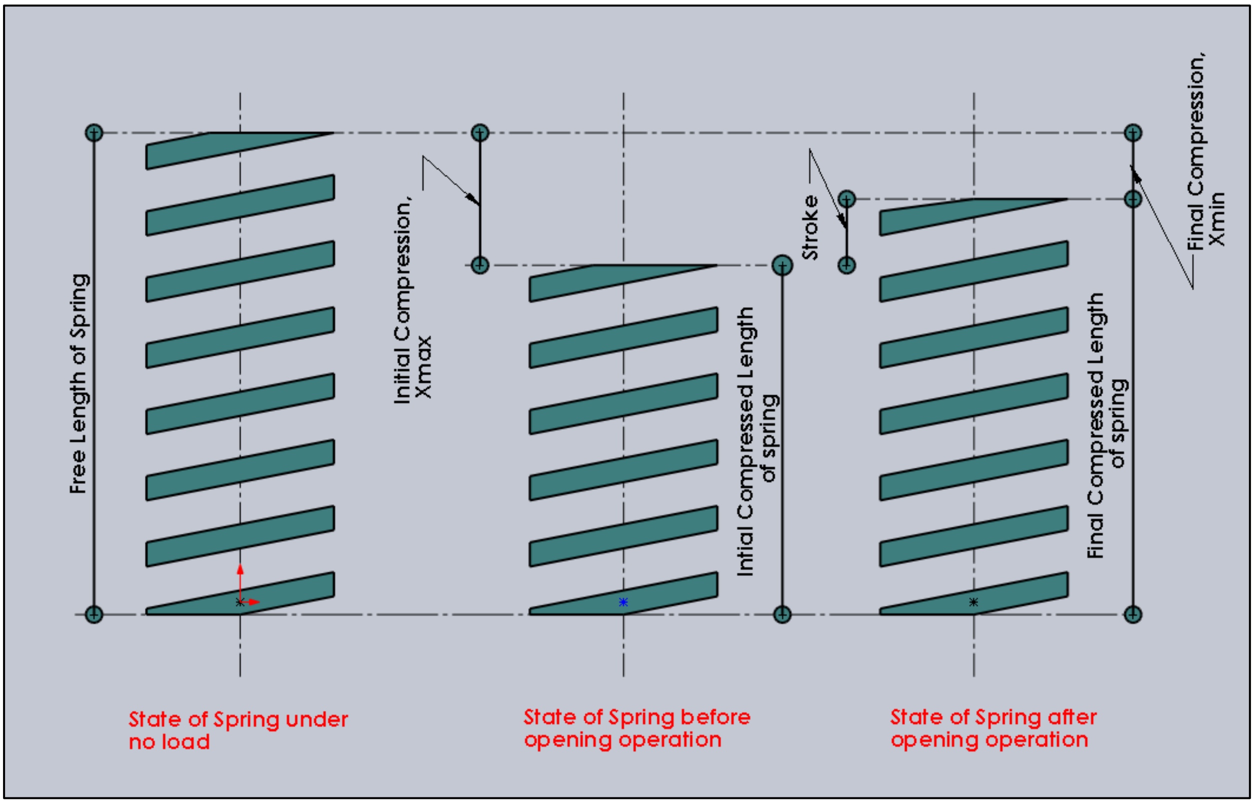

Figure 39: State of the spring during opening operation

Calculation for spring energy released during opening operation for the simplified model is shown in the following steps

Initial compression, $Xmax$

$$Xmax = \ \ Free\ Length - Intial\ compressed\ Length$$

Final compression, $Xmin$

$$Xmin = \ \ Xmax - Stroke$$

Min spring Force, $Fmin$

$$Fmin = \ k\ Xmin$$

Spring Energy released, E

$$E\ = 0.5\ k\ (\ Xmax^2 - \ Xmin^2)$$

5.7.2. CALCULATION OF FREE LENGTH OF THE SPRING FOR NEW VALUE OF STIFFNESS

The value of spring energy released, E in case of simplified model was now known to us. The value of stiffness, k was increased in steps and corresponding free length was calculated keeping spring energy released and stroke same in all the cases. Calculation for free length of the spring for new value of stiffness is given as follows

As stated above

$$E\ = 0.5\ k\ (\ Xmax^2 - \ Xmin^2)$$

$$Stroke = Xmax - Xmin$$

Therefore

$$\frac{E}{0.5\ \times k\ \times stroke} = Xmax + Xmin$$

$$Stroke = Xmax - Xmin$$

Taking same value for E and stroke as defined in section 5.7.1., and then Solving above 2 equations can result in the new value of Xmax and Xmin for a new value of k, stiffness. Once the values of Xmax and Xmin are calculated, new values of maximum spring force, minimum spring force and free length are calculated as

$$Fmin = \ k\ Xmin$$

$$Fmax = \ k\ Xmax$$

Keeping the value of initial compressed length same in all the cases, Value for free length for a new value of stiffness is given as

$$Free\ Length = Xmax + Intial\ compressed\ Length$$

Max spring force cannot exceed 44 kN as spring may fail beyond that load so therefore all the possible options for stiffness and free length are presented in the table 5.

Case. no	Stiffness, *K*, N/mm	Free Length, mm	Initial Compression, *Xmax*, mm	Final Compression, *Xmin*, mm	Max Spring Force, kN	Min Spring Force, kN	Spring energy released , kJ	Stroke, mm
1	201.3	589.6	212.6	92.6	42.8	18.6	3.6	120
2	221.3	575.8	198.8	78.8	44	17.4	3.6	120

Table 5: Different possible combinations for spring

5.7.3. RESULTS FOR WIPE TIME FOR DIFFERENT STIFFNESS

Results for wipe time for different value stiffness and their corresponding free length are presented in the table 6 below.

Case. no	K, Stiffness, N/mm	Free Length, mm	Wipe Time, milli second
1	171.3	616.3	15.2
2	201.3	589.6	14.8
3	221.3	575.8	14.6

Table 6: All the possible stiffness and Free Length values

As seen from the table, an increase in value of stiffness by 30 N/mm resulted in the reduction of 2.6 % in the wipe time. Likewise, increase in value of stiffness by 50 N/mm brought about a reduction of 3.9 % in the wipe time.

The reason for reduction in wipe time with increase in stiffness is explained below. Refer Fig 40.

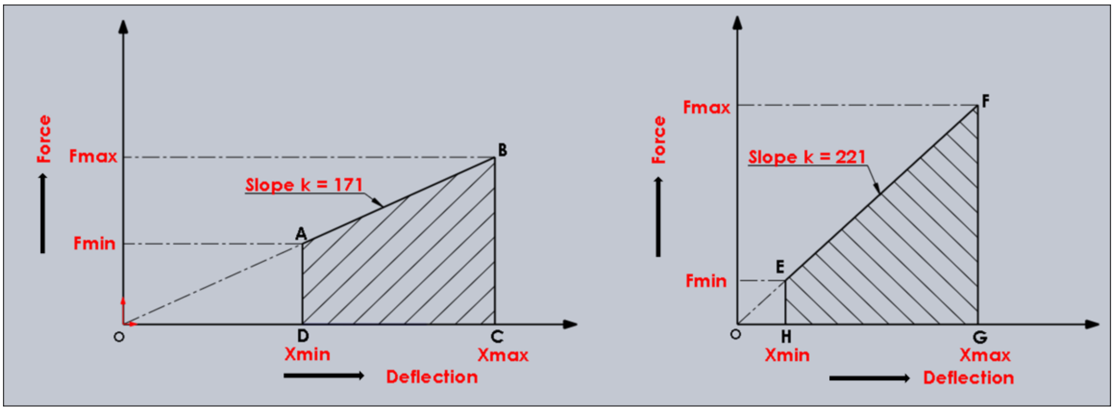

Figure 40: Graphical explanation for reduction in wipe time

Since energy released by the spring is same in all the cases, so therefore Energy released

$$Energy\ released, E = Area\ ABCD = Area\ EFGH$$

However with increase in stiffness, the average spring force required for opening of contacts has increased resulting in higher acceleration. Hence time required for opening of contacts gets reduced.

5.8. EFFECT OF LINKAGE DIMENSTION

Varying linkage dimension can affect the wipe time. Therefore we need to identify those dimensions of the linkages in the mechanism that can help in the minimization of the wipe time.

5.8.1. IDENTIFICATION OF LINKAGE DIMENSIONS

List of all the possible dimensions whose variation can cause minimization of wipe time are presented as follows.

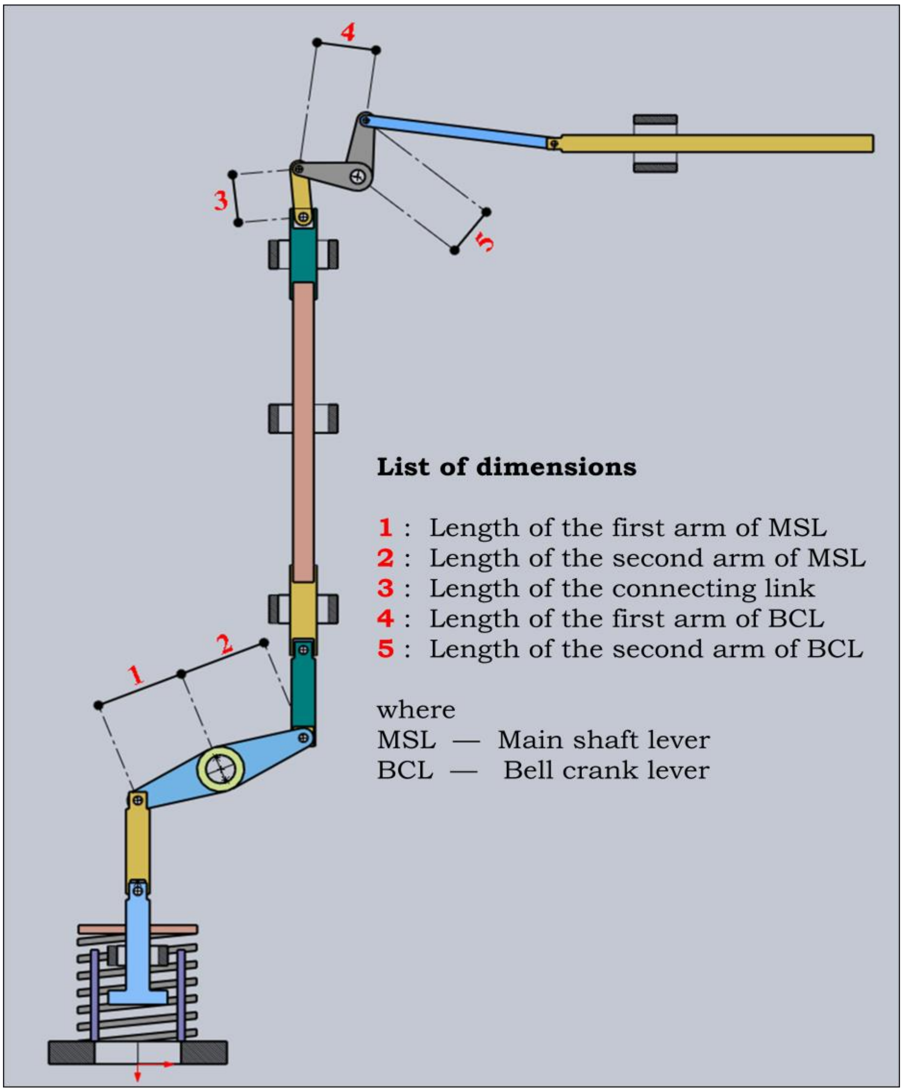

Figure 41: All the possible dimensions effecting wipe time

a. Length of the second arm of MSL
b. Length of the connecting link
c. Length of the first arm of BCL

These dimensions are marked in figure 41.

Variations in these dimensions are confined with the set of constraints. List of constraints are

a. Mechanism is designed in such a manner such that

$$R1 \times R2 = \frac{140}{120}$$

where

$$R1 = \frac{L2\_MSL}{L1\_MSL}$$

$L1\_MSL$ is the length of the first arm of MSL (Figure 41)

$L2\_MSL$ is the length of the second arm of MSL (Figure 41)

$$R2 = \frac{L2\_BCL}{L1\_BCL}$$

$L1\_BCL$ is the length of the first arm of BCL

$L2\_BCL$ is the length of the second arm of BCL

140 and 120 are respective stroke of the moving pole link and the spring.

b. Length of the first arm of MSL is held constant.

c. Stroke of the moving pole link and spring cannot change.

5.8.2. EFFECT OF LENGTH OF SECOND ARM OF MSL

From the simulation results, it was reported that wipe time is directly proportional to the length of the second arm of MSL. Wipe time decreases with decrease in the length of second arm of MSL.

Below Table 7 gives the values of wipe time for different length of the second arm of MSL.

Case number	Stiffness, N/mm	L1_MSL, mm	L2_MSL, mm	L1_BCL, mm	L2_BCL, mm	Wipe time, milli second
1	171.30	156.8	156.8	157.1	183.2	15.2
2			166.8		172.2	15.6
3			146.8		195.7	14.8
4			136.8		210.0	14.4

Table 7: Effect of second arm of MSL on wipe time

As seen from the table, as the length of the second arm of MSL, L2_MSL was increased by 10 mm, there was an increment of 2.6 % in the wipe time. Likewise a decrease of 10 mm in the length of the second arm of MSL resulted in the decrease of 2.6 % in the wipe time. Similarly reduction of 20 mm in the length of the second arm of MSL had led to a decrement of 5.26 % in wipe time.

5.8.3. EFFECT OF LENGTH OF THE FIRST ARM OF BCL

Table 8 clearly reflects the trend between wipe time and length of the first arm of BCL.

Case number	Stiffness, N/mm	L1_MSL, mm	L2_MSL, mm	L1_BCL, mm	L2_BCL, mm	Wipe time, milli second
1	171.3	156.83	156.83	157.1	183.2	15.2
2				166.1	193.8	15.2
3				175.1	204.2	15.4
4				151.1	176.2	15.2
5				145.1	169.2	15.2
6				139.1	162.2	15

Table 8: Effect off Length of the first arm of BCL on wipe time

When the length of the first arm of BCL, L1_BCL is increased by 18 units, 1.3 % rise in wipe time is reported from simulated results. On the other hand when the length of the first arm of BCL is decreased by 18 units, 1.3 % reduction in wipe time is reported. However the variation in wipe time with the change in dimension of first arm of BCL is minimal.

5.8.4. EFFECT OF LENGTH OF CONNECTING LINK

Table 9 clearly depicts the effect of length of connecting link on the wipe time.

Case .no	Stiffness, N/mm	L1_MSL, mm	L2_MSL, mm	L1_BCL, mm	L2_BCL, mm	Length of connecting Link, mm	Wipe time, milli second
1	171.3	156.8	156.8	157.1	183.2	130	15.2
2						112	15.2
3						100	15.4
4						154	15
5						166	14.8
6						194	14.4

Table 9: Effect of Length of connecting link on wipe time

From the simulated results, decrease in the length of connecting link by 30 mm has resulted in 1.3 % increase in the wipe time. On the other hand when the length of the connecting link is increased by 64 mm, 5.2 % reduction in the wipe time is reported.

5.8.5. EFFECT OF COMBINATION OF ALL PARAMETERS

In this case, effect of all the parameters on the wipe time is taken into consideration. Table 10 reflects those best values which led to minimization in wipe time.

Parameter Name	Value	Wipe time, milli second
Mass of the moving pole link	13.9	12.8
Mass of the pull rod	14.6	
Stiffness of the spring	221.3	
L2_MSL	136.8	
L1_BCL	157.1	
Length of connecting link	194	

Table 10: Effect of all the dimensions on wipe time

It is seen from the table 10 that with the suitable changes in the above parameters, wipe time reduced from 15.2 mille seconds to 12.8 mille seconds thus a reduction of 15.8 % in the wipe time.

CHAPTER 6

EFFECT OF FLEXIBILTY ON THE WIPE TIME

6.1. INTRODUCTION

In the previous chapters, while performing multi body dynamic simulation for a simplified model, all linkages were assumed as rigid bodies. Practically no link is considered as a perfectly rigid body as some amount of deformation occurs in every link. However In some links deformation is so small that it can be neglected but in case of pull rod link which is connected between operating mechanism and interrupter, experiment results have revealed large elastic deformations that cannot be ignored. Material used for pull rod is an insulating material such as plastics or its composites. The only limitation with insulating material is that phenomenon of anelasticity is observed in these material. In anelasticity, elastic deformation is not only a function of load applied but also time. Therefore in actual practice pull rod behaves as a flexible material. Flexibility in the pull rod may influence the wipe time and hence its effect needs to be studied.

6.2. EFFECT OF FLEXIBILITY IN THE PULL ROD

Flexible body dynamics was performed in ABAQUS for original simplified model in order to account for flexibility in the pull rod. Figure 42 below shows an FEA model.

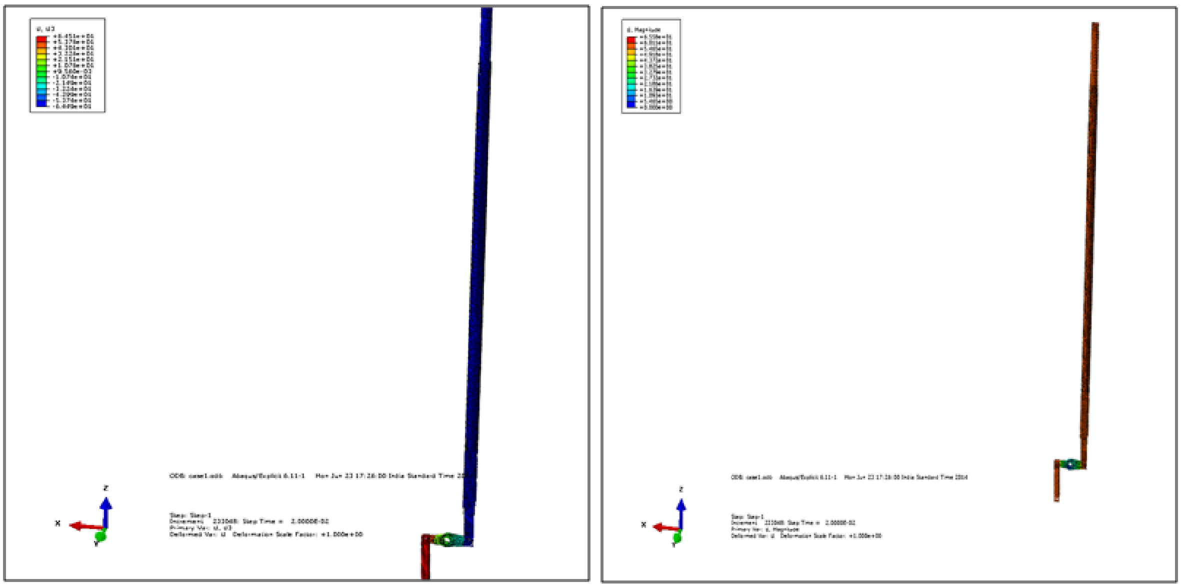

Figure 42: FEA Model to account for flexibility in pull rod

Once the flexibility was introduced in the pull rod, displacement curve for the top and bottom ends of pull rod, for the complete circuit breaker operation were obtained as output from the ABAQUS simulated results. Figure 43 below shows the graph of the displacement curves for pull rod top and bottom end when flexibility was introduced in the pull rod.

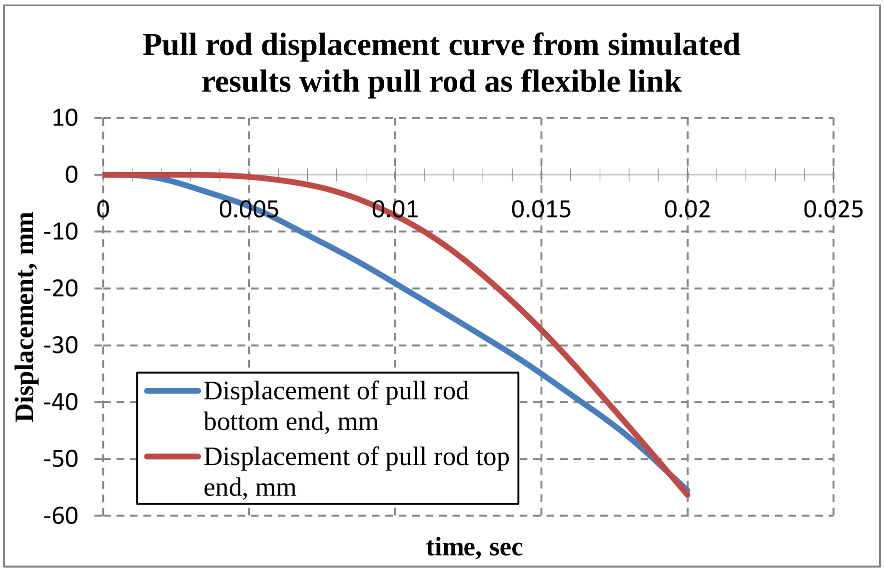

Figure 43: Pull rod displacement curve for flexible model from simulated results

As seen from the above figure 43, there is dissimilarity in the displacement curve for the top and bottom end of the pull rod because of flexibility in the pull rod. If pull rod had been assumed as a rigid link, then these two displacement curve would have been similar thus overlying on one another as shown in figure 44.

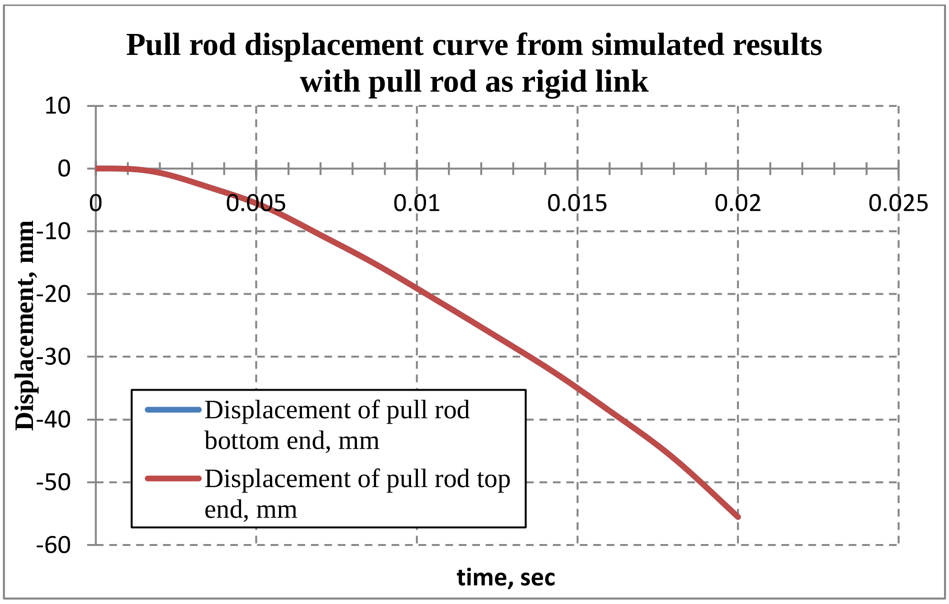

Figure 44: Pull rod displacement curve for rigid model from simulated results

These simulated results for flexible pull rod, figure 43 were then verified with the experimental results. Figure 45 shows the displacement curves for the top and bottom end of the flexible pull rod obtained from experimental results.

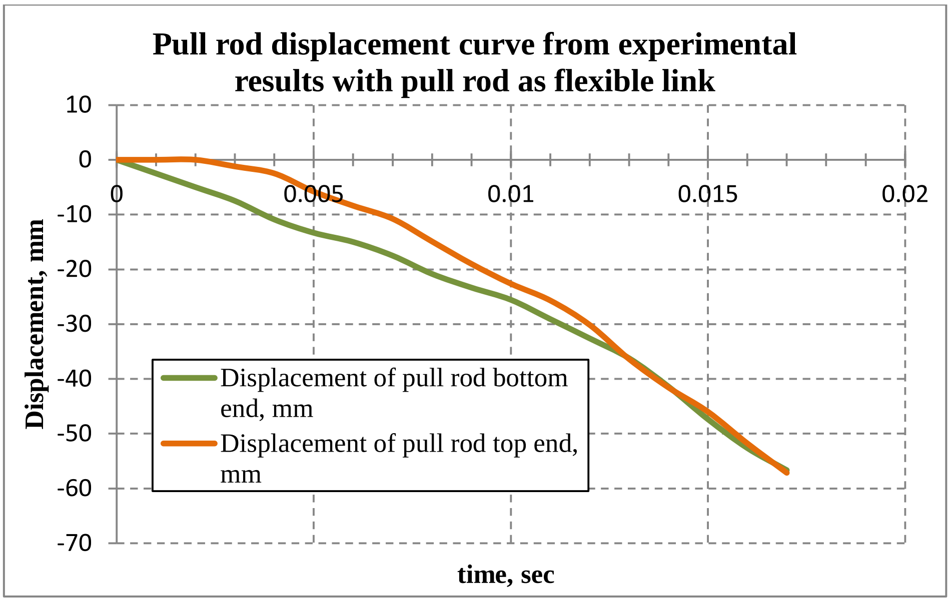

Figure 45: Pull rod displacement curve for flexible model from experimental results

As stated, wipe time is time for 35 mm travel by the pole moving link. An assumption was made that all the links above pull rod top end such as pull rod upper link, connecting link, BCL, pole_BCL_Link and moving pole link will be considered as perfectly rigid link, Refer figure 25. With this assumption, time taken for 35 mm travel by the pole moving link (Wipe time) was same as 35 mm travel by the pull rod top end.

For rigid pull rod

$$\begin{aligned} wipe\ time &= time\ taken\ for\ 35\ mm\ travel\ by\ pull\ rod\ top\ end \\ &= time\ taken\ for\ 35\ mm\ travel\ by\ pull\ rod\ bottom\ end \end{aligned}$$

For flexible pull rod

$$\begin{aligned} wipe\ time &= time\ taken\ for\ 35\ mm\ travel\ by\ pull\ rod\ top\ end \\ &\neq time\ taken\ for\ 35\ mm\ travel\ by\ pull\ rod\ bottom\ end \end{aligned}$$

Therefore it was concluded that flexibility in the pull rod led to dissimilar displacement curve for top and bottom end of the pull rod thus effecting the wipe time. In order to obtain an accurate value for wipe time, flexibility in the pull rod need to be taken into consideration. Our next task was to measure the elastic constant of the flexibility pull rod and further study the effect of improved stiffness on the wipe time.

6.3. TENSILE TESTING

Tensile testing for pull rod was carried out on a universal testing machine (UTM). Material used for pull rod was fiber reinforced plastics (FRP). Three samples of pull rod were tested. Load was applied gradually in steps and corresponding deflection was recorded. The specification for Universal testing machine is presented in the table 11 below.

Parameter name	Value	Units
Maximum Capacity	600	kN
Principle of operation	Hydraulic	—
Power	2.5	HP
L x W x H	2265 x 750 x 2534	mm

Table 11: Specification for UTM

Figure 46 shows the Universal testing machine on which test was carried out.

Figure 46: Universal testing machine

The samples were made as per ASTM D- 2015, Standard test method for longitudinal tensile properties of fiberglass pipe and tube. Figure 47, 48, 49 shows the images of the failed samples after tensile testing. Failure in the specimen occurred when slippage in the threaded connection was observed.

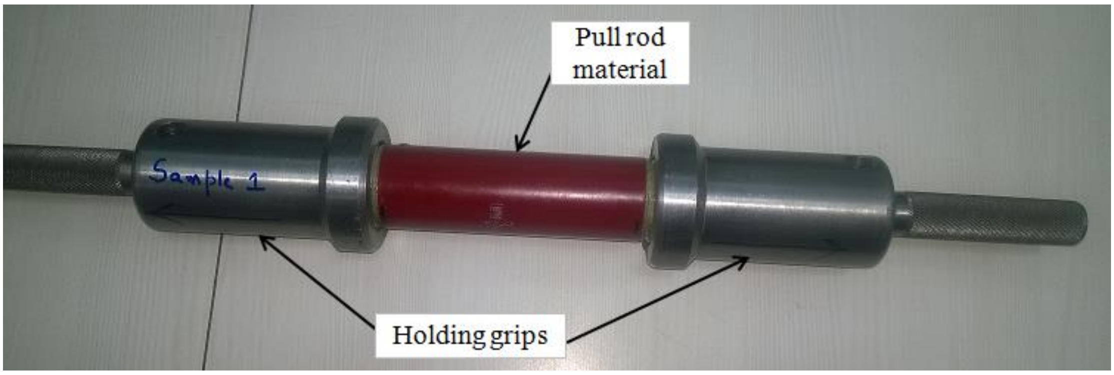

Figure 47: Sample 1 of the pull rod

Figure 48: Sample 2 of the pull rod

Figure 49: Sample 3 of the pull rod

Once the load, deflection data was obtained for three samples, stress strain curve was further plotted as shown in the figure 50 below.

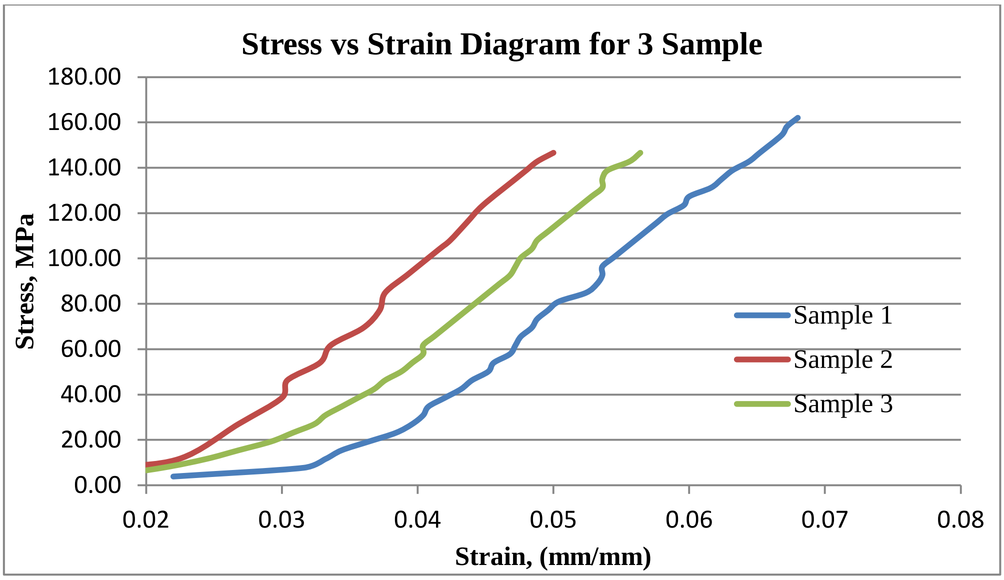

Figure 50: Stress Strain Curve for 3 samples

The value of young modulus, E obtained from the graph was approximately 5234.3 N/mm^2. Load per unit deflection was given as

$$Load\ per\ unit\ deflection = \frac{A\ \times E}{l}$$

Where A is original cross sectional area of the pull rod

E is young modulus

L is original length of the specimen

Area and length of the specimen were known to us and the value of load per unit deflection (Stiffness) was given as 10.8 kN / mm.

Once the value of elastic constant was known to us, our next task was to consider the effect of improved stiffness on the wipe time which is considered as a future scope of project.

CHAPTER 7

CONCLUSION AND FUTURE WORK

7.1. CONCLUSION

In this thesis, performance of a circuit breaker mechanism was improved by minimizing the wipe time. Parameters that could influence the wipe time were identified as

a. Stiffness of the spring
b. Linkage dimension
c. Mass of the pull rod and moving pole link

Individual effect of these parameters on the wipe time was studied. From the simulated results it was reported that wipe time could be reduced by

a. Increasing the stiffness of the spring
b. Reducing the mass of the pull rod and moving pole link
c. Varying linkage dimension suitably to minimize wipe time

When the combined effect of all the parameters was taken into consideration, simulated results reported a 15.8 % of reduction in the wipe time and an equivalent reduction of 22.9% in the opening time.

Effect of flexibility on the wipe time was also studied in this thesis. Pull rod was considered as a flexible material. By introducing flexibility, both the simulated and experimental results reported that there was dissimilarity in the displacement curves for the two ends of the pull rod thus effecting the wipe time. Therefore it was concluded that an accurate value of wipe time would be obtained only if flexibility is introduced in the pull rod. An attempt to measure the elastic constant for the flexible pull rod was then made. The value for young modulus was given as 5234.3 N/mm^2 and load per unit deflection (Stiffness) was 10.8 kN / mm.

7.2. FUTURE WORK

As stated in the conclusion part, a correct prediction for wipe time will be obtained only if flexibility is introduced in the pull rod. Future work of this thesis is then to obtain that correct value for wipe time. This can be done only if we study the effect of improved stiffness (10.8 kN / mm) on the wipe time. Accounting for friction in revolute and sliding joints during the modeling phase would also give an added advantage for correct prediction of wipe time. Therefore, for modeling this physical problem closer to reality, it becomes necessary that the effect of flexibility and friction must be taken into account.

REFERENCES

[1] Fu-Chen Chen, and Yih-Fong Tzeng, “On the dynamics of spring-type operating mechanism for 69 KV SF6 gas insulated circuit breaker in open operation”, *Computers & Structures*, Volume 80, Issue 22, September 2002, Pages 1715–1723

[2] Gyuseok Choi, Jeonghyun Sohn, Hyunwoo Kim, Wansuk Yoo, Byungtae Bae, Jaeyeol Kim, and Jinho Kim, “Performance improvement of a gas-insulated circuit breaker using multibody dynamic simulations and experiments”, *Journal of Mechanical Science and Technology,* November 2013, Volume 27, Issue 11, pp 3223-3229

[3] Sung Pil Jung, Kab Jin Jun, Tae Won Park, and Ill Chul Ahn, “An Optimum Design of a Gas Circuit Breaker Using Design of Experiments”, Mechanics *Based Design of Structures and Machines*, 36: 346–363, 2008

[4] Farid Al-Bender, “Fundamentals of Friction Modeling”, Proceedings, ASPE Spring Topical Meeting on Control of Precision Systems, MIT, April 11-13, 2010

[5] Janusz Frączek, and Marek Wojtyra, “On the unique solvability of a direct dynamics problem for mechanisms with redundant constraints and Coulomb friction in joints”, *Mechanism and Machine Theory,* Volume 46, Issue 3, March 2011, Pages 312–334

[6] M. Wojtyra, Joint reactions in rigid body mechanisms with dependent constraints, *Mechanism and Machine Theory,* Volume 44, Issue 12, December 2009, Pages 2265–2278

[7] Onesmus Muvengei, John Kihiu, and Bernard Ikau, “Computational implementation of LuGre Friction law in a revolute joint with clearance”, *Mechanical Engineering Conference on Sustainable Research and Innovation*, Volume 4, 3rd-4th May 2012

[8] Lankarani, H.M., and Nikravsh, P.E., “A contact force model with hysteresis damping for impact analysis of multibody systems,” *ASME J.Mech Des*., vol. 112, pp. 369-376, 1990.

[9] Enlai Zheng, and Xinlong Zhou, “Modeling and simulation of flexible slider-crank mechanism with clearance for a closed high speed press system”, *Mechanism and Machine Theory*, Volume 74, April 2014, Pages 10–30

[10] M-S. Claessens, L. Drews4, R. Govindarajan, M. Holstein, H. Lohrberg, and P. Robin-Jouan, “Advanced Modeling Methods for Circuit Breakers”, CIGRE 2006

WEB REFERENCES

1. http://en.wikipedia.org/wiki/File:Jtecul.jpg
2. http://en.wikipedia.org/wiki/Circuit_breaker
3. http://www05.abb.com/global/scot/scot245.nsf/veritydisplay/26886facea44b7b1c1257cec0046a07c/$file/1HSM%209543%2023-02en%20Live%20Tank%20Circuit%20Breaker%20-%20Application%20Guide%20Ed1.2.pdf
4. http://2.bp.blogspot.com/-PASeCsem3F0/T26HOCI1jRI/AAAAAAAACBw/yNLV_c_5BPU/s1600/DSC00068-002.JPG
5. http://www.electrical4us.com/electrical-switchgear-and-theory-of-switchgear-protection/
6. http://4.bp.blogspot.com/--R_KwUfcyqI/T05k6ZndknI/AAAAAAAAAx4/O6854c5AA94/s1600/SF6BreakerWorkingPrinciple.jpg
7. https://s3-eu-west-1.amazonaws.com/productdatasheets/Circuit%20Breaker%20Testing%20Guide_3586.pdf
8. http://www.ewh.ieee.org/soc/pes/switchgear/presentations/2003-1_Thu_3_Hermosillo.pdf
9. https://bib.irb.hr/datoteka/364758.DCIGRE_WG_A306_Intermediate_Results_Circuit_Breakers_1.pdf
10. http://books.google.co.in/books?id=VCrXlrRW0TsC&pg=PA107&lpg=PA107&dq=pneumatic+mechanism+circuit+breaker&source=bl&ots=Ghc0N51XQm&sig=QxnsIKOvIKoXD3cZx10FNBOq7yc&hl=en&sa=X&ei=LsSFU82OJ5ePuASqs4LYCQ&ved=0CCIQ6AEwAQ#v=onepage&q=pneumatic%20mechanism%20circuit%20breaker&f=false